

# 深層学習の実際

現在の中心的な技術は  
多層ニューラル  
ネットワーク

しかも2次元で  
多層ニューラル  
ネットワーク

# ネオコグニトロン

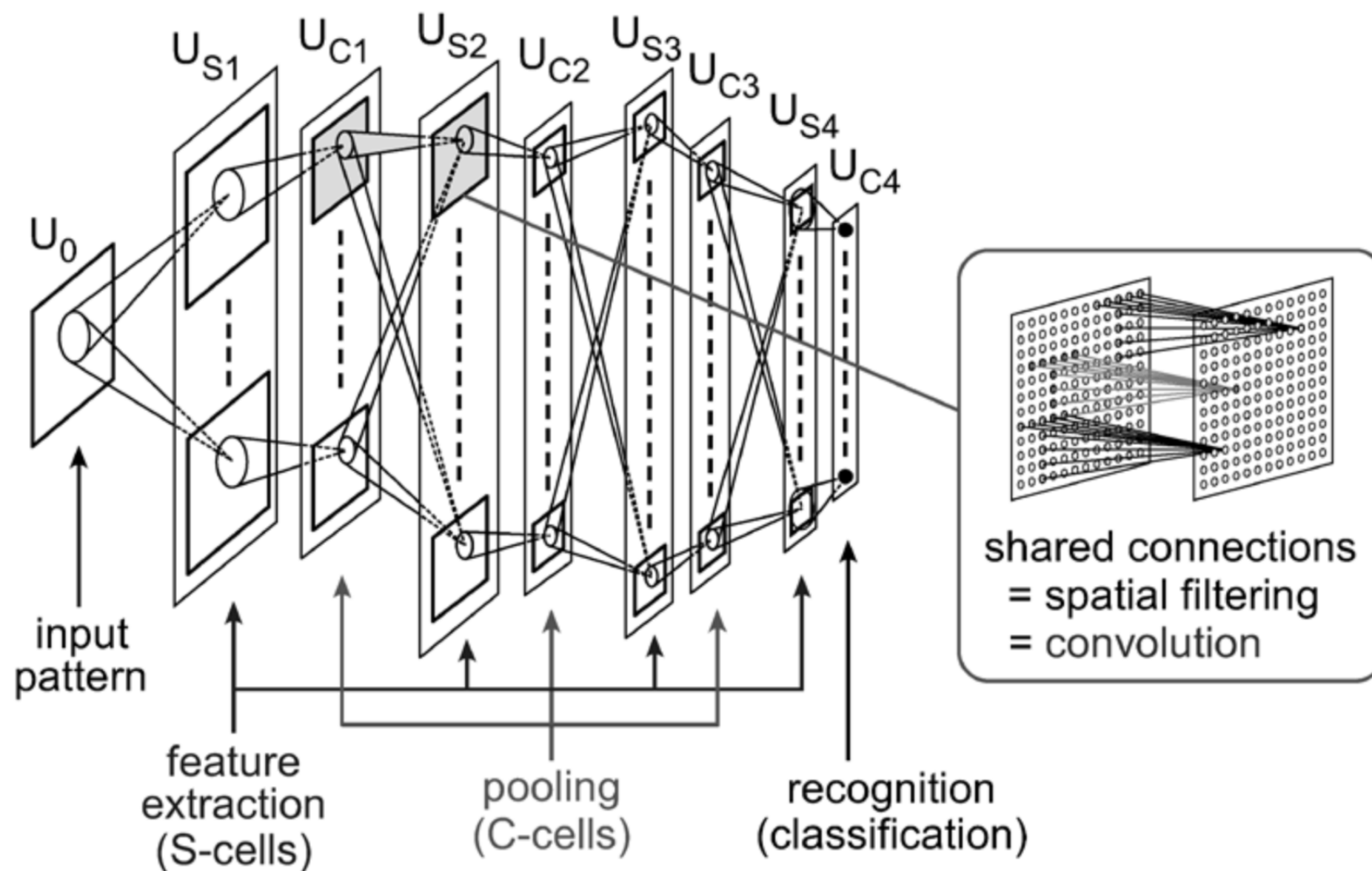


図1 ネオコグニトロンの回路構造.

# ネオコグニトロン

## 画像を直接入力

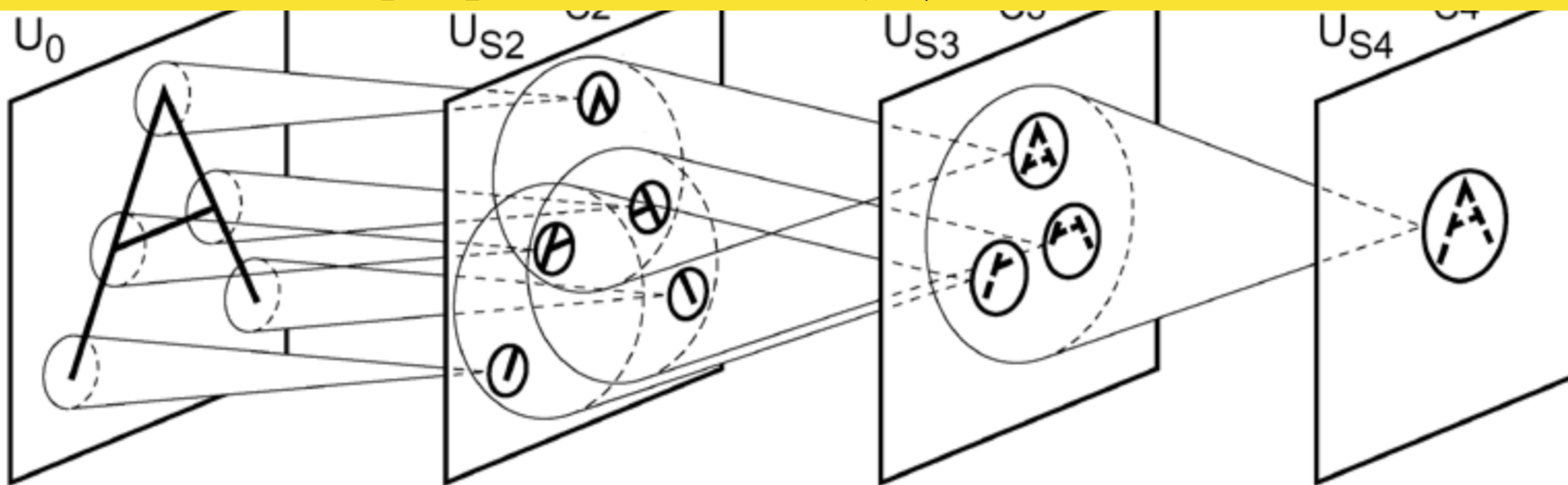


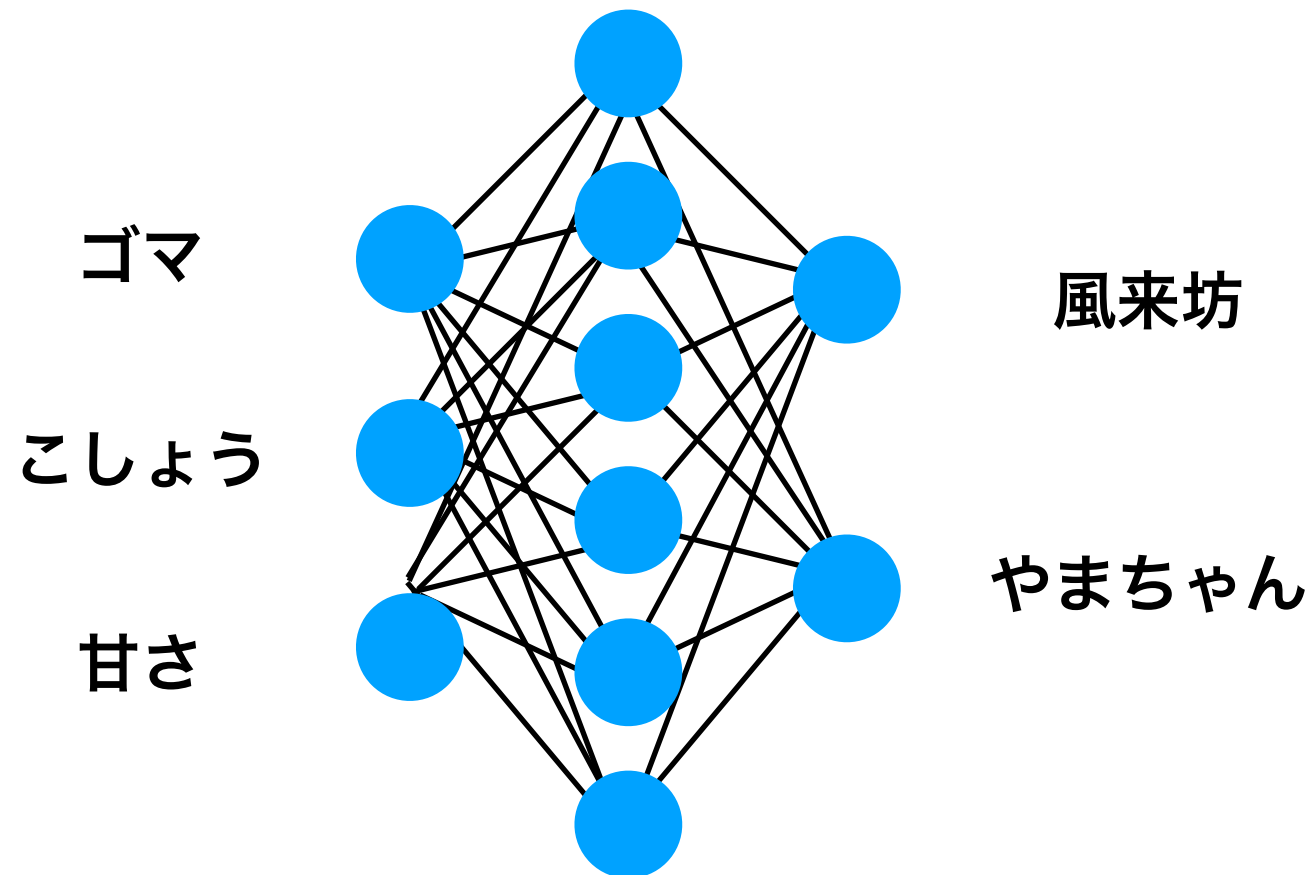
図2 ネオコグニトロンにおけるパターン認識の原理<sup>1)</sup>

# 名古屋は「手羽先」だがや



## 山ちゃん or 風来坊 自動判別

# 従来技術



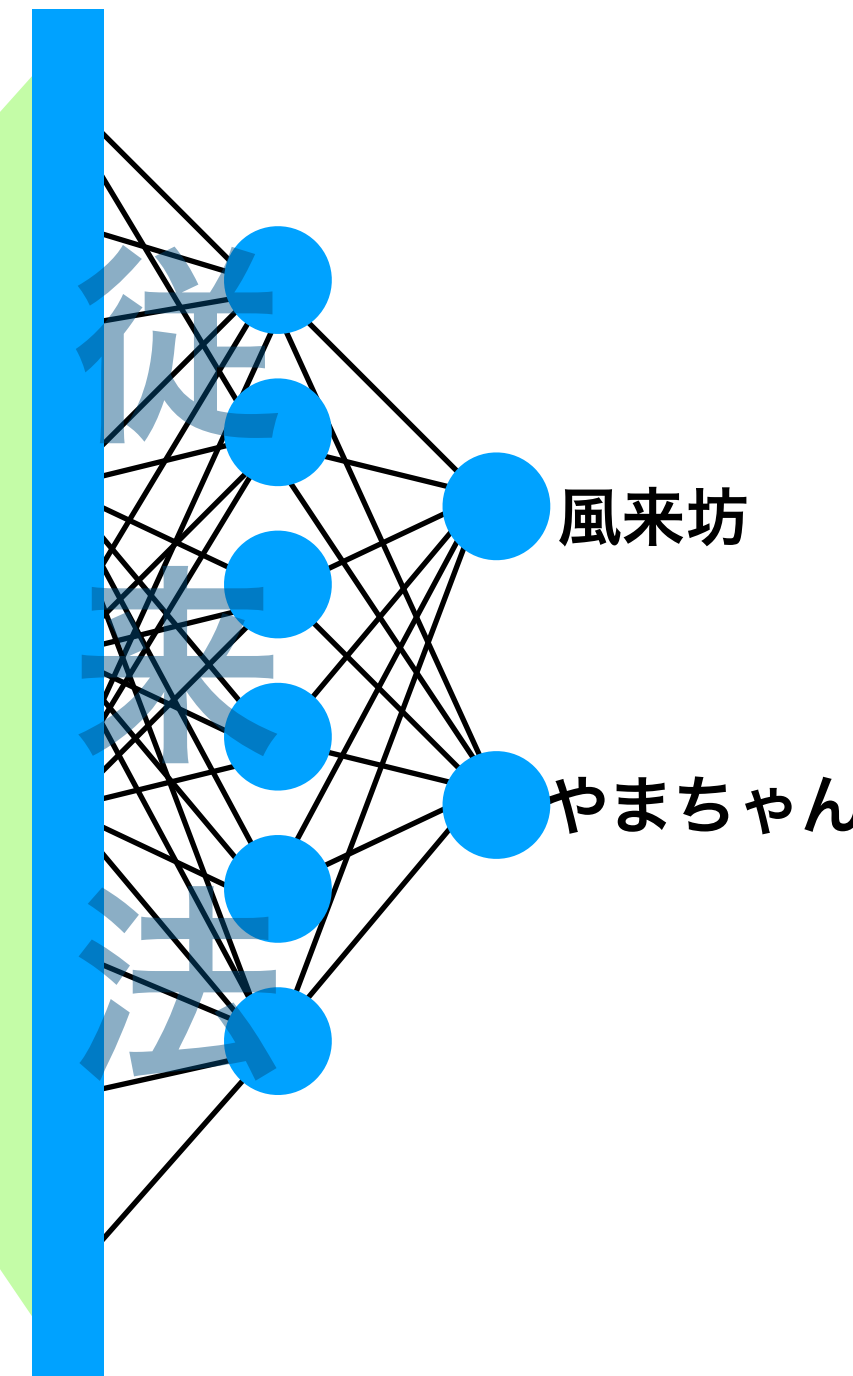
# 特徴を手動で抽出

# どう変わったか？



置  
み込  
みNN

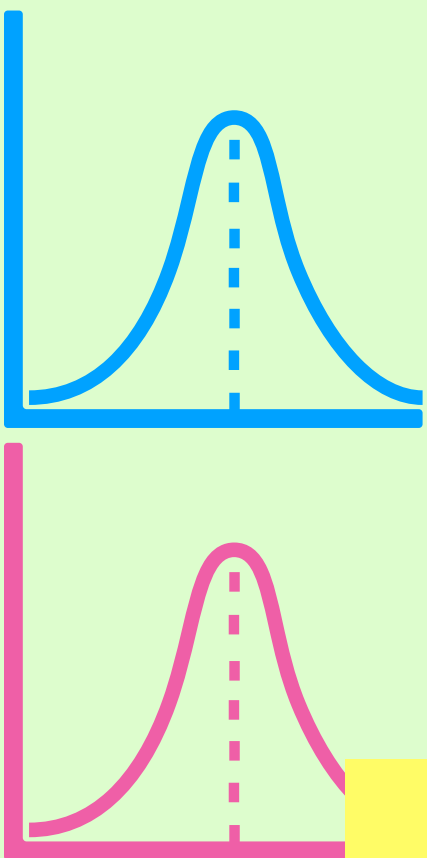
(CNN)



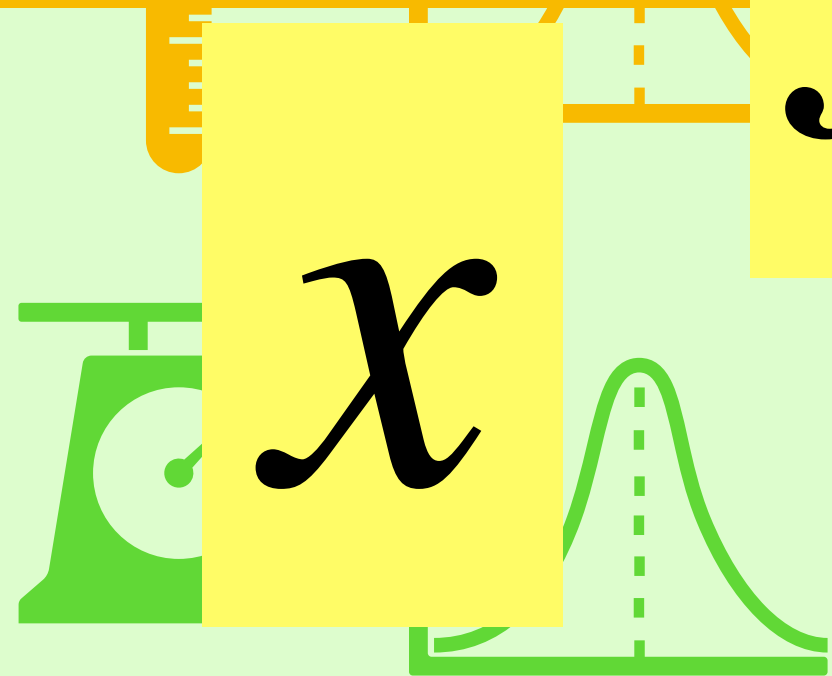
## 画像を直接入力

深層學習

考え方



説明変数



$f$  関数

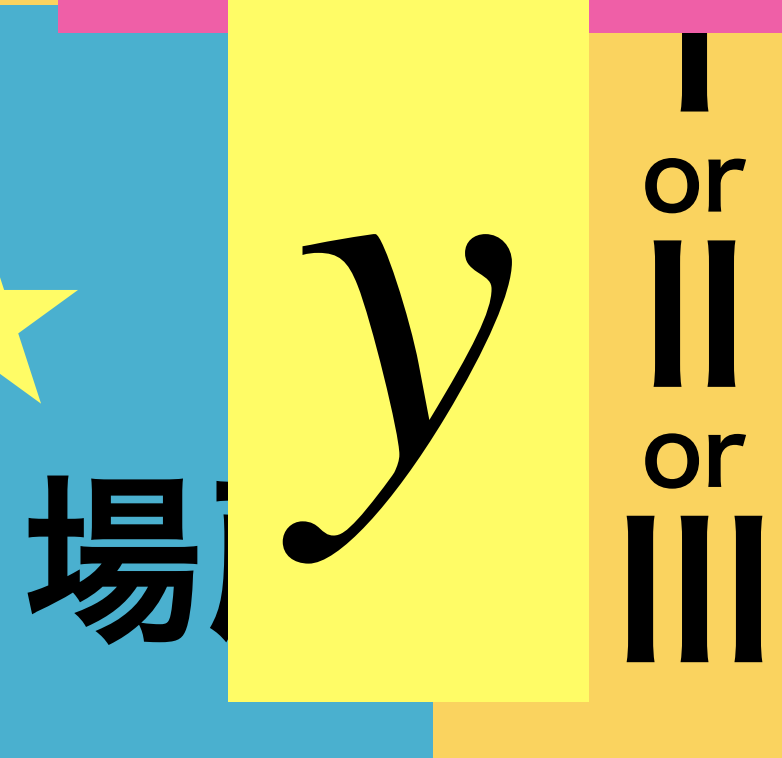
深層

学習

数值



目的変数



# $x, y$ で関数を決める

学習とはコレを  
決定すること

機械学習で獲得

$y$

目的変数

(群／数値)

$f(x)$

説明変数

(ベクトル)

教師あり学習

関数っていろいろあったなあ～

$$f(x) = ax^2 + bx + c \quad \text{モデル}$$

ちょっとだけ一般化

$$f(x, \theta), \quad \theta = \{a, b, c\} \quad \text{パラメタ}$$

# 学習データと評価データ

- 性能評価のためには検証が必要

学習とはコレを  
決定すること

機械学習で獲得

 $y$ 

目的変数

(群／数値)

 $f(x)$ 

説明変数

(ベクトル)

教師あり学習

$f$ を構築するためのデータ：学習データ／Trainingデータ

その後に評価するためのデータ：評価データ／Testデータ

学習データと評価データが混ざるといわゆる「カンニング」

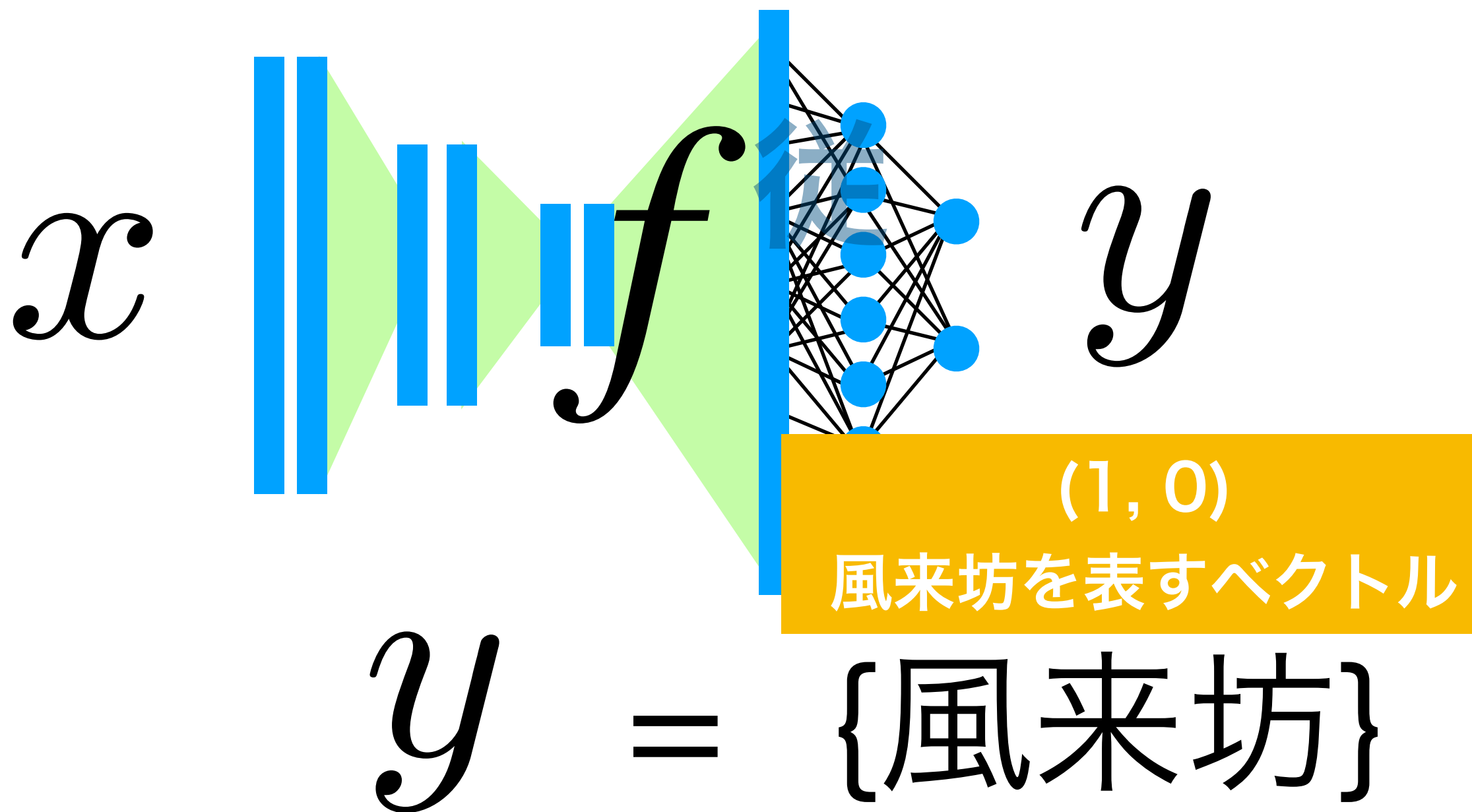
混ざらないように かつ 少ないデータを最大限活用する工夫

Cross-validation/Leave-one-outなど

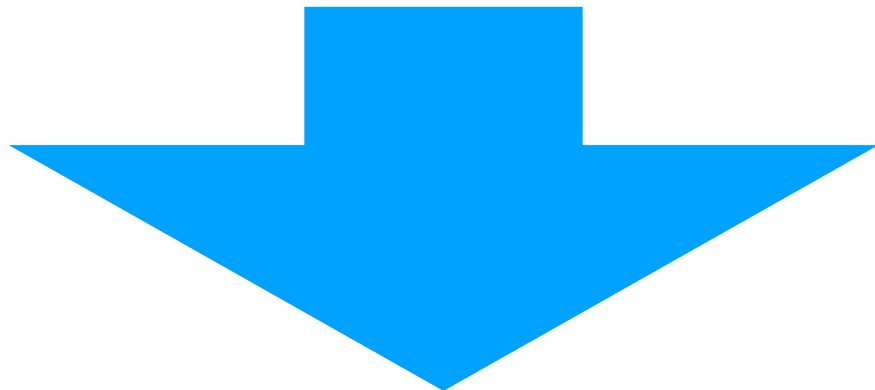
$x =$



画像も音声も文字  
もすべて数値データ



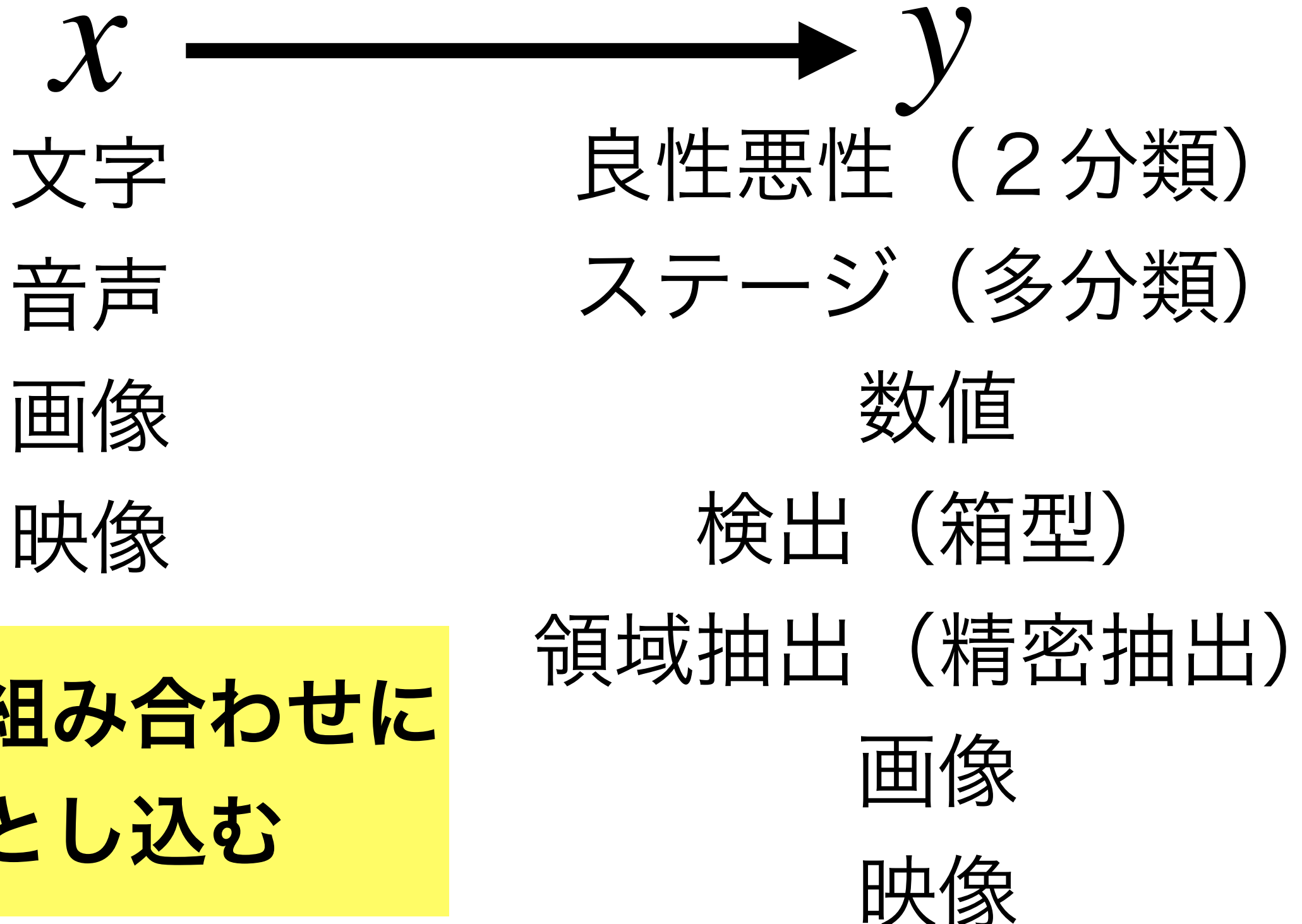
ディープラーニングを使う



$x, y$  に何を持ってくるか？

ディープラーニングは  
与えられた  $x, y$   
に従って関数を決定する

# ディープラーニングを使う



# 画像分野での代表的な問題

検出 四角で検出

領域分割 精密に抽出

分類 2クラス／多クラス

推定 回帰

画質改善 ノイズ除去, 被ばく低減

画像生成 フェイク画像生成

データ抽出 異常検知（教師なし学習）

データと正解があれば

自動で学習

じゃどのくらい？

## ORIGINAL RESEARCH

# A Deep Learning Approach for Assessment of Regional Wall Motion Abnormality From Echocardiographic Images



Kenya Kusunose, MD, PhD,<sup>a</sup> Takashi Abe, MD, PhD,<sup>b</sup> Akihiro Haga, PhD,<sup>c</sup> Daiju Fukuda, MD, PhD,<sup>a</sup> Hirotugu Yamada, MD, PhD,<sup>a</sup> Masafumi Harada, MD, PhD,<sup>b</sup> Masataka Sata, MD, PhD<sup>a</sup>

## ABSTRACT

**OBJECTIVES** This study investigated whether a deep convolutional neural network (DCNN) could provide improved detection of regional wall motion abnormalities (RWMA) and differentiate among groups of coronary infarction territories from conventional 2-dimensional echocardiographic images compared with that of cardiologists, sonographers, and resident readers.

**BACKGROUND** An effective intervention for reduction of misreading of RWMA is needed. The hypothesis was that a DCNN trained using echocardiographic images would provide improved detection of RWMA in the clinical setting.

**METHODS** A total of 300 patients with a history of myocardial infarction were enrolled. From this cohort, 3 groups of 100 patients each had infarctions of the left anterior descending (LAD) artery, the left circumflex (LCX) branch, and the right coronary artery (RCA). A total of 100 age-matched control patients with normal wall motion were selected from a database. Each case contained cardiac ultrasonographs from short-axis views at end-diastolic, mid-systolic, and end-systolic phases. After the DCNN underwent 100 steps of training, diagnostic accuracies were calculated from the test set. Independently, 10 versions of the same model were trained, and ensemble predictions were performed using those versions.

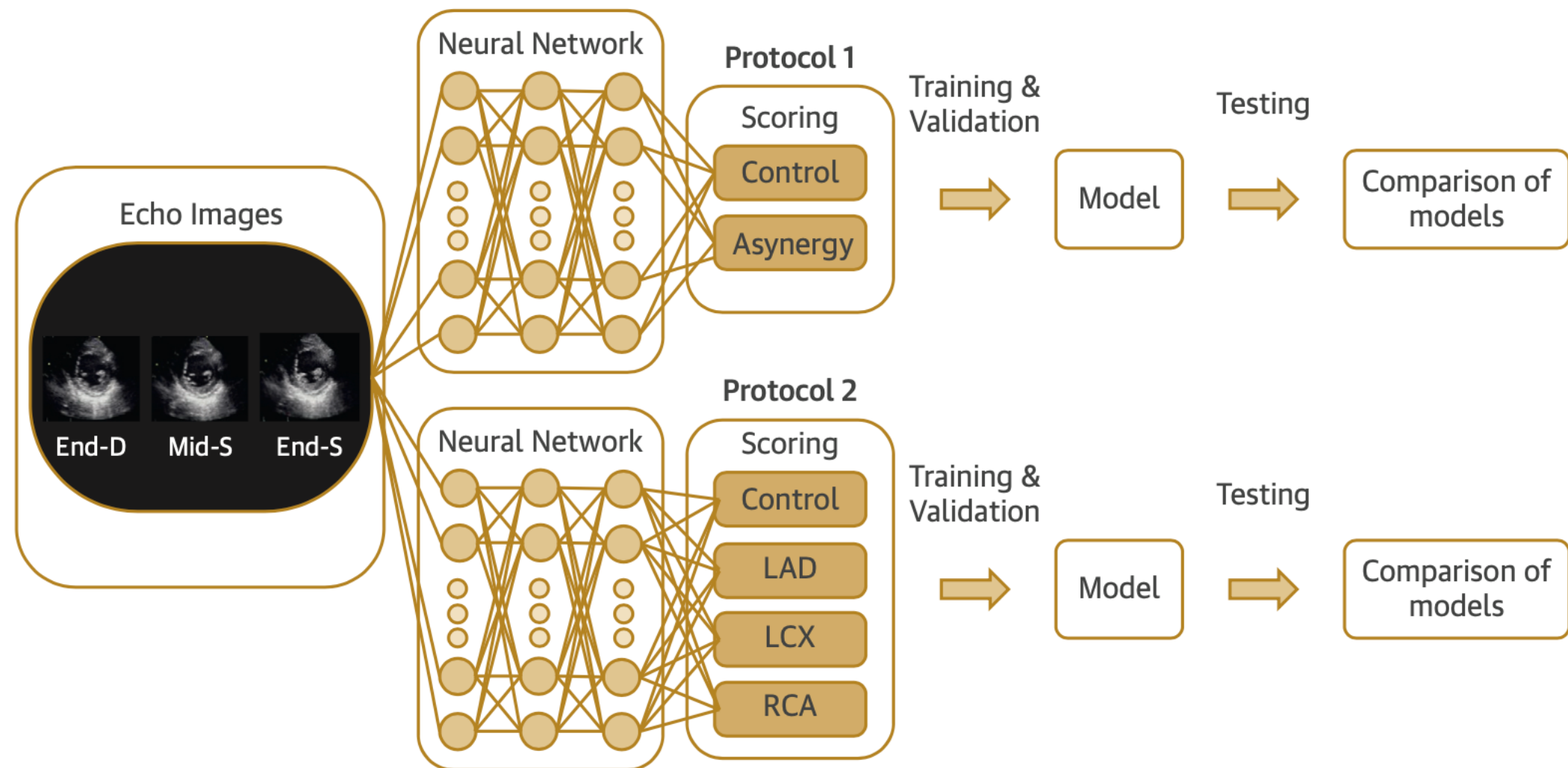
X  
超音波画像 3 枚

y  
局所壁運動

異常の有無  
(2 分類)

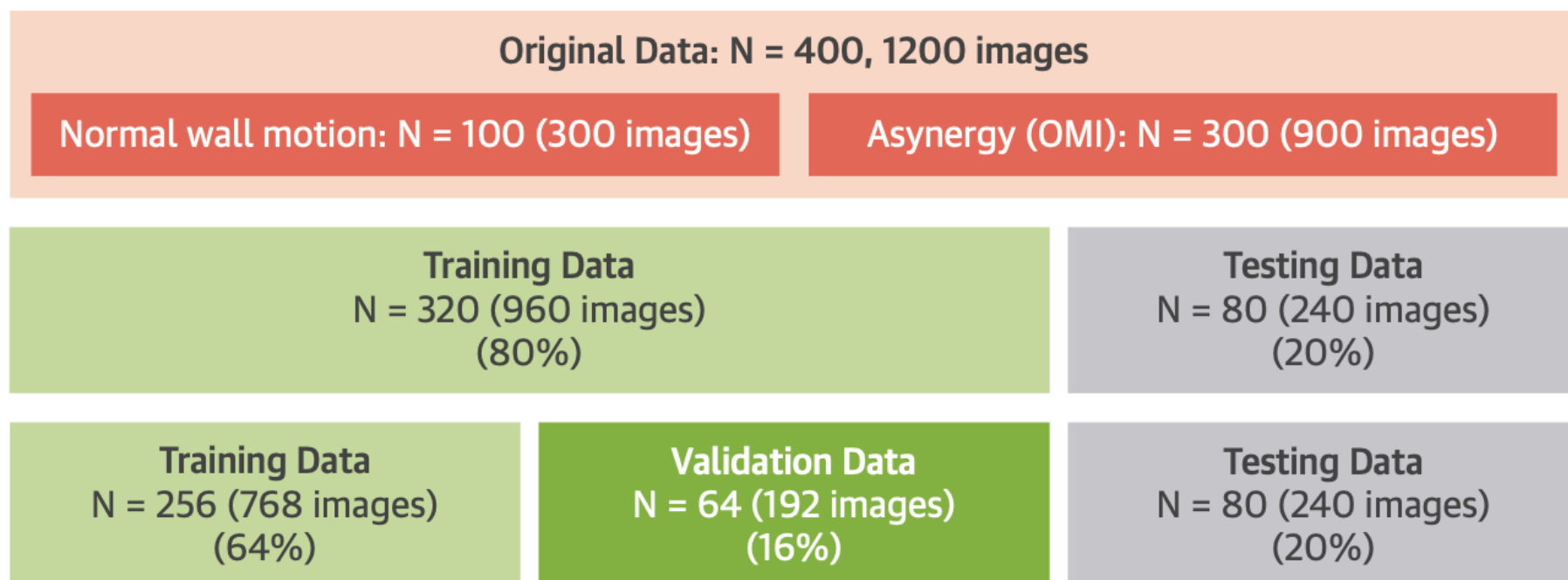
$n = 300$

## CENTRAL ILLUSTRATION Neural Networks for the Presence of RWMA<sup>s</sup> and the Territory of RWMA<sup>s</sup>



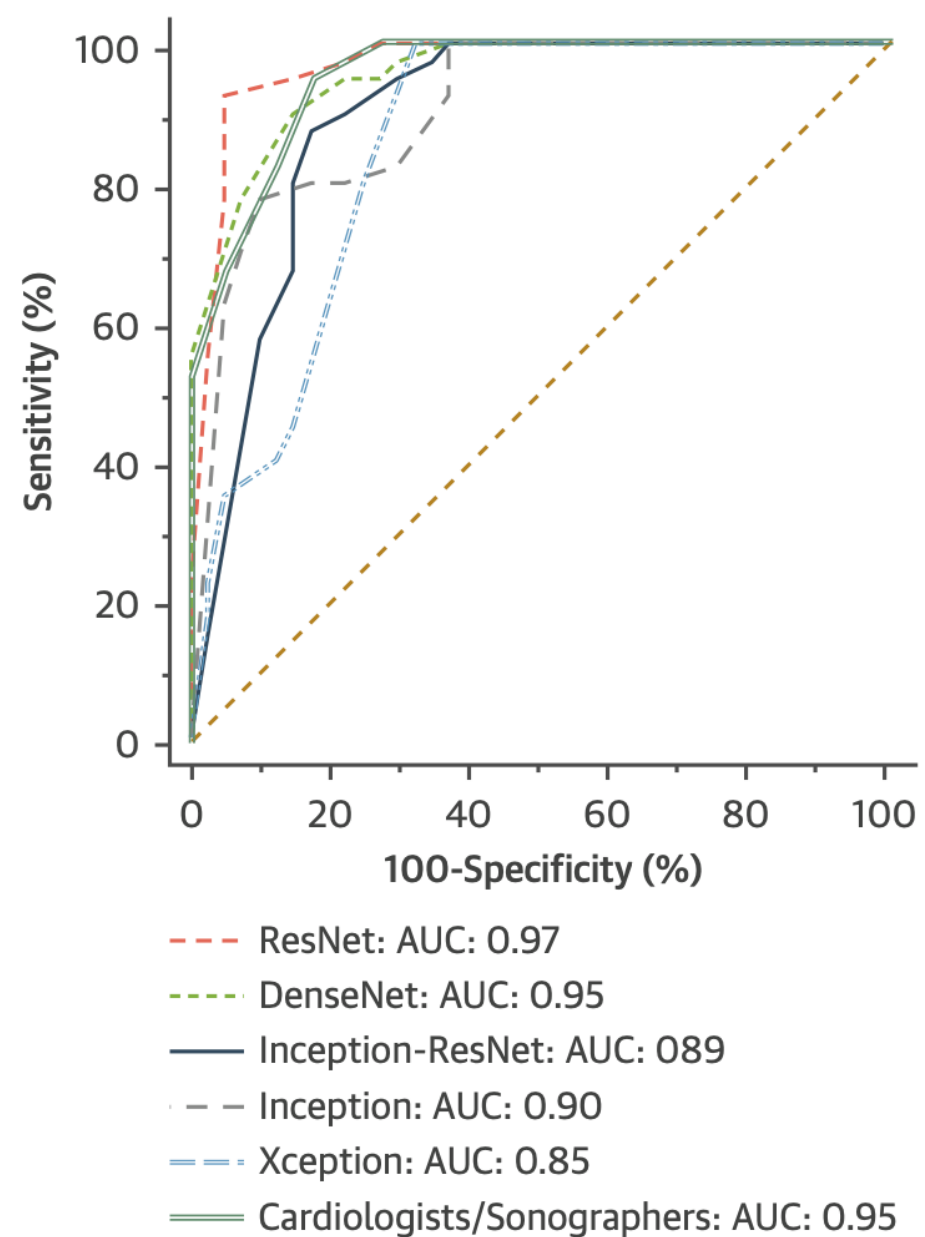
Kusunose, K. et al. J Am Coll Cardiol Img. 2020;13(2):374-81.

The fully connected layers transform the image features into the final scores by adjusting weights for neuron activations during training. Echo = echocardiography; End-D = end diastolic (phase); LAD = left anterior descending artery; LCX = left circumflex artery; Mid/End-S = mid-/end systolic (phases); RCA = right coronary artery; RWMA = regional wall motion abnormality.

**FIGURE 1 Import Data**

There were a total of 400 cases from which 1,200 images were split with 256 cases (786 images) as the training set, 64 cases (192 images) as the validation set, and 80 cases (240 images) as the test set. OMI = old myocardial infarction.

**FIGURE 3 Diagnostic Ability to Detect the Presence of RWMA**s



The area under the curves by several deep learning algorithms for detection of territories of wall motion abnormality were good. AUC = area under the curve; ResNet = residual neural network; other abbreviation as in [Figure 2](#).

## ORIGINAL RESEARCH ARTICLE



# Fully Automated Echocardiogram Interpretation in Clinical Practice Feasibility and Diagnostic Accuracy

Editorials, see p 1636 and p 1639

**BACKGROUND:** Automated cardiac image interpretation has the potential to transform clinical practice in multiple ways, including enabling serial assessment of cardiac function by nonexperts in primary care and rural settings. We hypothesized that advances in computer vision could enable building a fully automated, scalable analysis pipeline for echocardiogram interpretation, including (1) view identification, (2) image segmentation, (3) quantification of structure and function, and (4) disease detection.

**METHODS:** Using 14 035 echocardiograms spanning a 10-year period, we trained and evaluated convolutional neural network models for multiple tasks, including automated identification of 23 viewpoints and segmentation of cardiac chambers across 5 common views. The segmentation output was used to quantify chamber volumes and left ventricular mass, determine ejection fraction, and facilitate automated determination of longitudinal strain through speckle tracking. Results were evaluated through comparison to manual segmentation and measurements from 8 666 echocardiograms obtained during the routine clinical workflow. Finally, we developed models to detect 3 diseases: hypertrophic cardiomyopathy, cardiac amyloid, and pulmonary arterial hypertension.

Jeffrey Zhang, BA  
Sravani Gajjala, MBBS  
Pulkit Agrawal, PhD  
Geoffrey H. Tison, MD,  
MPH  
Laura A. Hallock, BS  
Lauren Beussink-Nelson,  
RDCS  
Mats H. Lassen, BM  
Eugene Fan, MD  
Mandar A. Aras, MD, PhD  
ChaRandle Jordan, MD,  
PhD  
Kirsten E. Fleischmann,  
MD, MPH  
Michelle Melisko, MD  
Atif Qasim, MD, MSCE  
Sanjiv J. Shah, MD  
Ruzena Bajcsy, PhD  
Rahul C. Deo, MD, PhD

$x$   
超音波画像 1 枚  
 $y$   
分割画像  
多クラス分類

$n = 14035$

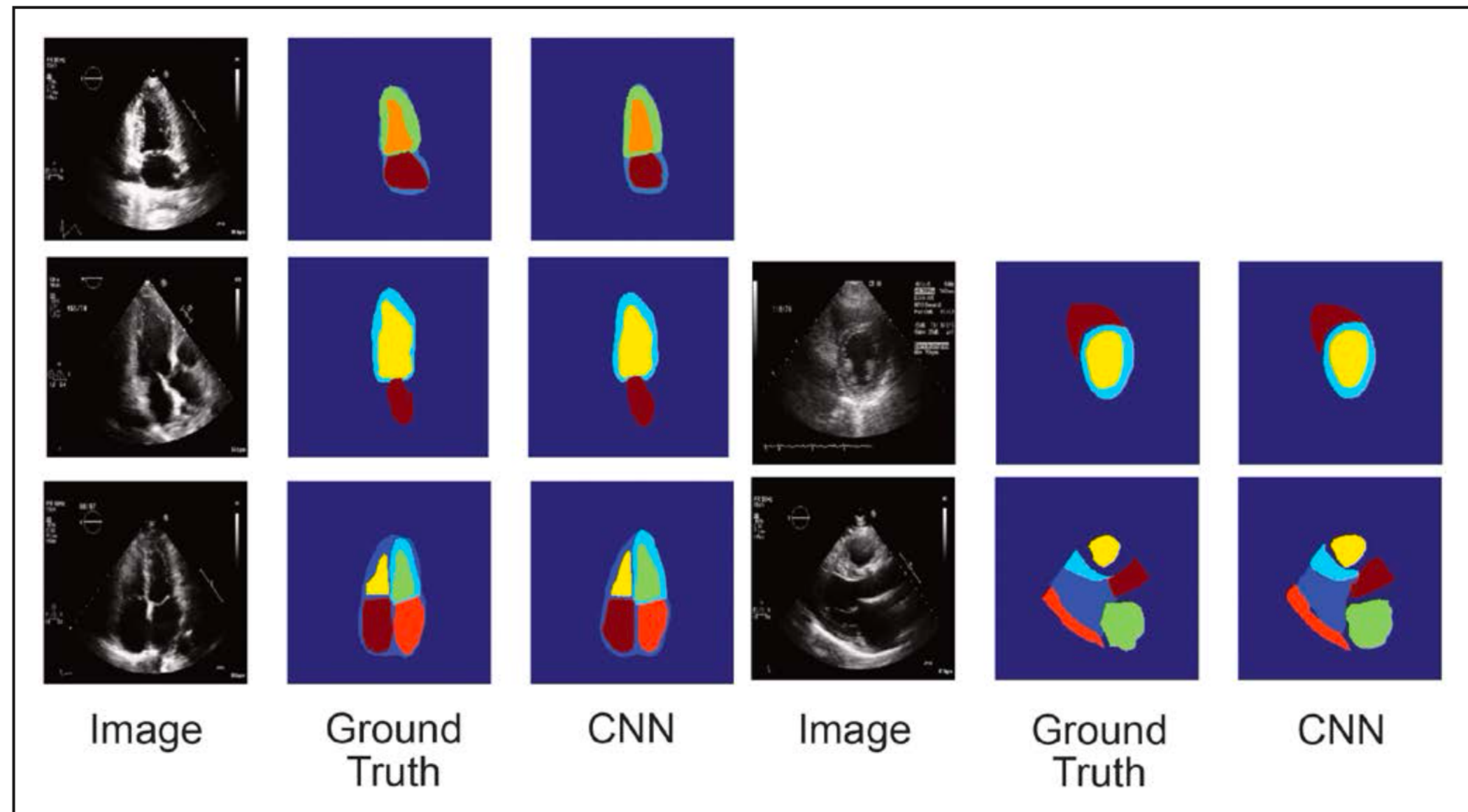


**Figure 3. Convolutional neural networks successfully segment cardiac chambers.**

We used the U-net algorithm to derive segmentation models for 5 views: A2c, A3c, A4c (left: top, middle, and bottom, respectively), parasternal short axis at the level of the papillary muscle (right, middle), and PLAX (right, bottom). For each view, the trio of images, from left to right, corresponds to the original image, the manually traced image used in training (ground truth), and the automated segmented image (determined as part of the cross-validation process). A2c indicates apical 2-chamber; A3c, apical 3-chamber; A4c, apical 4-chamber; CNN, convolutional neural network; and PLAX, parasternal long axis.

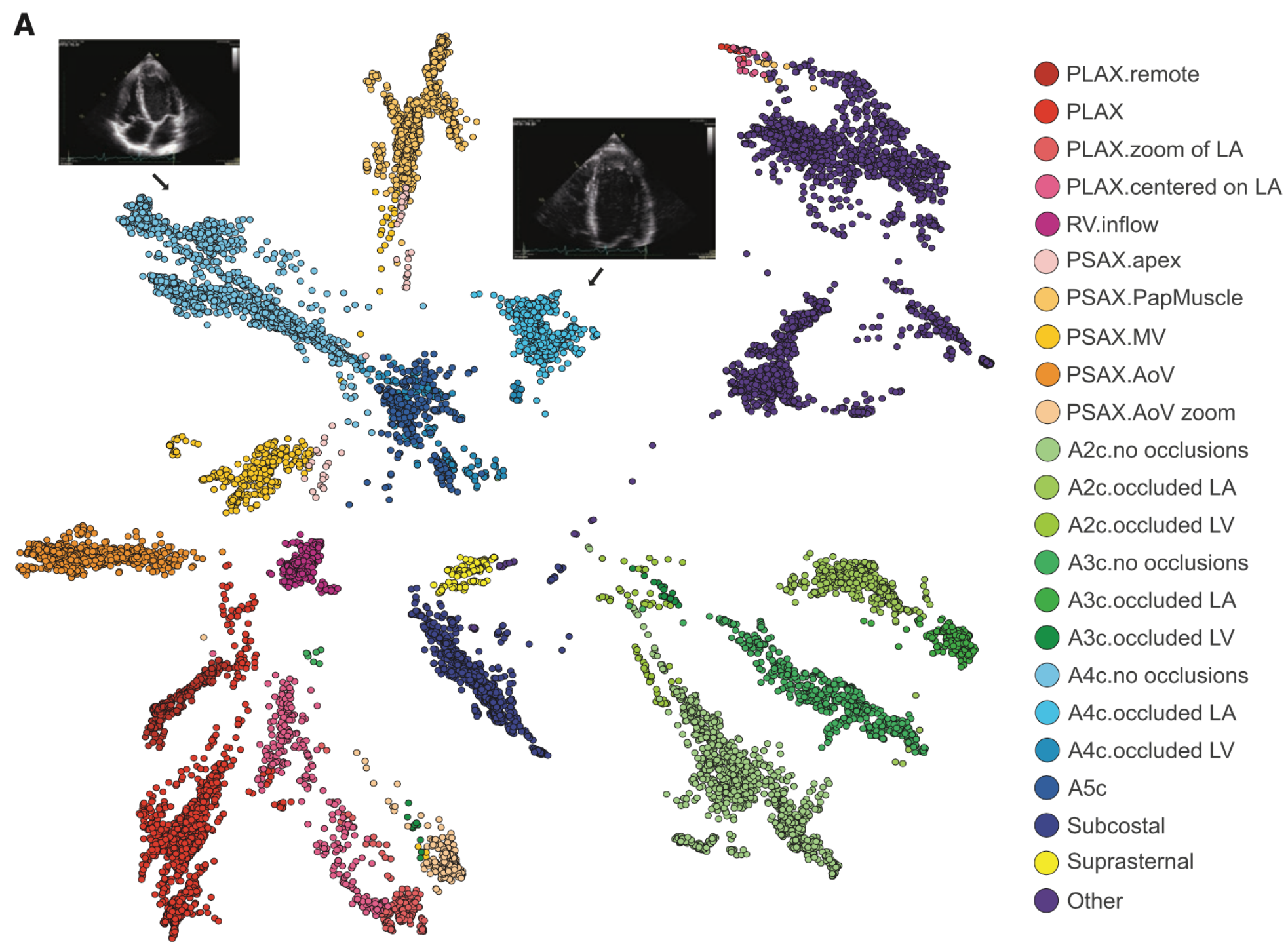


**Figure 2. Convolutional neural networks successfully discriminate echocardiographic views.**

**A**, t-Distributed Stochastic Neighbor Embedding (t-SNE) visualization of view classification. t-SNE is an algorithm used to visualize high-dimensional data in lower dimensions. It depicts the successful grouping of test images corresponding to 23 different echocardiographic views. Echocardiographic still images indicate the distinct clustering of images of A4c views without occlusions and those with occlusion of the left atrium. **B**, Confusion matrix demonstrating successful and unsuccessful view classifications within the test data set. Numbers along the diagonal represent successful classifications, whereas off-diagonal entries are misclassifications. A2c indicates apical 2-chamber; A3c, apical 3-chamber; A4c, apical 4-chamber; echo, echocardiogram; LV, left ventricular; and PLAX, parasternal long axis.

Zhang J, Gajjala S, Agrawal P, Tison GH, Hallock LA, Beussink-Nelson L, Lassen MH, Fan E, Aras MA, Jordan C, Fleischmann KE, Melisko M, Qasim A, Shah SJ, Bajcsy R, Deo RC. Fully Automated Echocardiogram Interpretation in Clinical Practice. Circulation. 2018 Oct 16;138(16):1623-1635. doi: 10.1161/CIRCULATIONAHA.118.034338. PMID: 30354459; PMCID: PMC6200386.

**B**

## Prediction of echo views for individual images

**Ground Truth**

	PLAX.remote	PLAX	PLAX.zoom of LA	PLAX.centered on LA	RV inflow	PSAX.apex	PSAX.PapMuscle	PSAX.MV	PSAX.AoV	PSAX.AoV zoom	A2c.no occlusions	A2c.occluded LA	A2c.occluded LV	A3c.no occlusions	A3c.occluded LA	A3c.occluded LV	A4c.no occlusions	A4c.occluded LA	A4c.occluded LV	A5c	Subcostal	Suprasternal	Other		
PLAX.remote	364	45	0	0	0	0	0	0	0	0	0	0	0	0	0	0	0	0	0	0	0	0	0	0	
PLAX	13	1155	10	82	3	0	1	0	27	0	0	9	0	10	1	0	0	0	0	0	0	0	0	0	
PLAX.zoom of LA	0	0	81	75	0	0	0	4	0	1	0	0	0	0	6	0	0	0	4	0	0	0	0	0	
PLAX.centered on LA	0	21	52	107	2	0	0	0	7	2	0	0	0	0	0	0	0	0	0	0	0	0	0	0	
RV inflow	0	18	4	18	266	2	15	2	8	0	7	0	0	0	1	0	5	0	0	0	0	0	0	0	
PSAX.apex	0	0	0	0	0	0	0	0	0	0	0	0	0	0	0	0	0	0	0	0	0	0	0	0	
PSAX.PapMuscle	0	17	0	0	41	26	936	129	13	2	1	10	0	0	0	0	19	21	0	2	0	1	0	0	
PSAX.MV	0	1	0	5	7	18	0	195	29	0	0	0	0	0	0	0	0	0	0	0	0	0	0	0	
PSAX.AoV	0	17	3	14	0	0	0	4	766	20	0	0	0	0	0	0	1	0	1	0	15	2	0	0	
PSAX.AoV zoom	0	0	29	1	0	0	1	8	39	290	0	0	0	0	4	0	0	0	3	13	0	0	0	0	
A2c.no occlusions	0	1	0	0	0	4	0	0	9	0	1070	90	36	80	8	0	38	17	0	23	2	0	0	0	
A2c.occluded LA	0	0	0	0	0	0	0	0	0	0	67	362	2	0	9	0	44	0	1	0	0	0	0	0	
A2c.occluded LV	0	0	0	0	0	0	0	2	0	0	64	0	10	0	0	0	1	0	10	0	0	0	0	0	
A3c.no occlusions	0	0	0	0	0	0	0	0	0	0	20	5	0	435	80	30	3	0	0	0	0	0	0	0	
A3c.occluded LA	0	0	0	0	0	0	0	0	0	0	1	3	12	21	161	0	0	1	0	0	0	0	0	0	
A3c.occluded LV	0	0	0	0	0	0	0	0	0	0	0	9	11	0	0	0	0	0	0	0	0	0	0	0	
A4c.no occlusions	0	0	0	0	0	0	2	0	0	90	1	0	0	0	0	0	1530	45	104	93	0	0	0	0	
A4c.occluded LA	0	0	0	0	0	3	0	0	0	22	32	0	0	0	0	0	28	543	20	12	0	0	0	0	
A4c.occluded LV	0	0	0	0	0	0	6	0	0	0	0	1	0	0	0	0	3	4	47	20	0	0	0	0	
A5c	0	0	0	0	0	0	0	0	0	0	0	0	0	0	0	0	14	0	9	185	0	0	0	0	
Subcostal	3	1	1	0	1	0	0	0	2	0	0	3	0	0	0	0	9	1	9	15	930	1	24	0	
Suprasternal	0	0	0	8	0	0	4	0	0	0	0	0	0	0	0	0	0	0	0	36	146	16	0	0	
Other	0	10	0	20	0	0	14	0	0	0	0	0	0	3	0	0	0	0	0	20	0	3255	0	0	0

## Predictions

**Figure 2. Convolutional neural networks successfully discriminate echocardiographic views.**

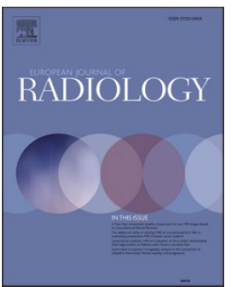
**A**, t-Distributed Stochastic Neighbor Embedding (t-SNE) visualization of view classification. t-SNE is an algorithm used to visualize high-dimensional data in lower dimensions. It depicts the successful grouping of test images corresponding to 23 different echocardiographic views. Echocardiographic still images indicate the distinct clustering of images of A4c views without occlusions and those with occlusion of the left atrium. **B**, Confusion matrix demonstrating successful and unsuccessful view classifications within the test data set. Numbers along the diagonal represent successful classifications, whereas off-diagonal entries are misclassifications. A2c indicates apical 2-chamber; A3c, apical 3-chamber; A4c, apical 4-chamber; echo, echocardiogram; LV, left ventricular; and PLAX, parasternal long axis.



Contents lists available at ScienceDirect

## European Journal of Radiology

journal homepage: [www.elsevier.com/locate/ejrad](http://www.elsevier.com/locate/ejrad)



# Artificial intelligence in ultrasound

Yu-Ting Shen<sup>a</sup>, Liang Chen<sup>b</sup>, Wen-Wen Yue<sup>a,\*</sup>, Hui-Xiong Xu<sup>a,\*</sup>

<sup>a</sup> Department of Medical Ultrasound, Shanghai Tenth People's Hospital, Ultrasound Research and Education Institute, Tongji University School of Medicine, Tongji University Cancer Center, Shanghai Engineering Research Center of Ultrasound Diagnosis and Treatment, National Clinical Research Center of Interventional Medicine, Shanghai, 200072, PR China

<sup>b</sup> Department of Gastroenterology, Shanghai Tenth People's Hospital, Tongji University School of Medicine, Shanghai, 200072, PR China



## ARTICLE INFO

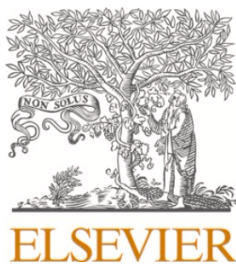
### Keywords:

Ultrasound  
Artificial intelligence  
Deep learning  
Medical imaging

## ABSTRACT

Ultrasound (US), a flexible green imaging modality, is expanding globally as a first-line imaging technique in various clinical fields following with the continual emergence of advanced ultrasonic technologies and the well-established US-based digital health system. Actually, in US practice, qualified physicians should manually collect and visually evaluate images for the detection, identification and monitoring of diseases. The diagnostic performance is inevitably reduced due to the intrinsic property of high operator-dependence from US. In contrast, artificial intelligence (AI) excels at automatically recognizing complex patterns and providing quantitative assessment for imaging data, showing high potential to assist physicians in acquiring more accurate and reproducible results. In this article, we will provide a general understanding of AI, machine learning (ML) and deep learning (DL) technologies; We then review the rapidly growing applications of AI-especially DL technology in the field of US-based on the following anatomical regions: thyroid, breast, abdomen and pelvis, obstetrics heart and blood vessels, musculoskeletal system and other organs by covering image quality control, anatomy localization, object detection, lesion segmentation, and computer-aided diagnosis and prognosis evaluation; Finally, we offer our perspective on the challenges and opportunities for the clinical practice of biomedical AI systems in US.

Shen YT, Chen L, Yue WW, Xu HX. Artificial intelligence in ultrasound. Eur J Radiol. 2021;139:109717. Epub 2021/05/08. doi: 10.1016/j.ejrad.2021.109717. PubMed PMID: 33962110.

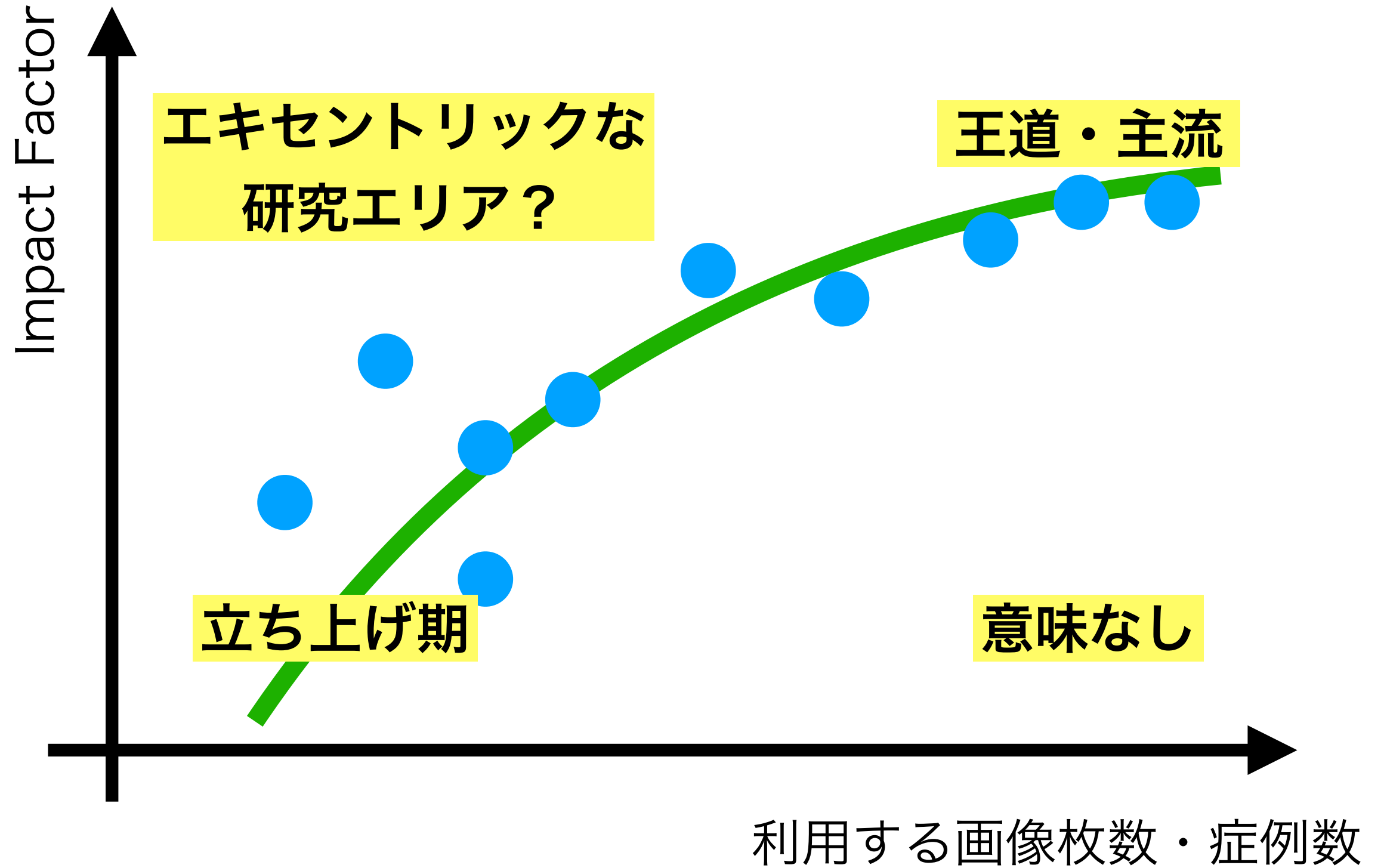
**Table 4**

Summarize the machine learning applications in heart and blood vessels and musculoskeletal system as well as other organ systems ultrasonic image analysis in the papers surveyed.

Organ system and body location	Disease classification	Object detection	Image segmentation	Prognosis evaluation
Heart	View classification of echocardiograms [99,100]	Detection of heart disease [98,103, 104]	Segmentation of the ventricle of the heart [105]	
	Classification of myocardial wall motion [101,102]		Segmentation of left ventricle and left atrium [106]	
	Diagnosis of ventricular volume [161]			
Blood vessels	Classification of carotid artery intima-media thickness [107]	Detection of vascular lumen [109]	Segmentation of lumen-intima and media-adventitia [110,111,112]	
	Characterization of plaque composition in vascular [108]		Segmentation of vascular structure [113]	
Musculoskeletal system	Diagnosis of myositis from muscle US [114]	US-assisted vertebral body positioning [116]	Segmentation of rectus femoris muscle [118]	
	Estimation of skeletal muscle status [115]	Detection and identification of spine level [117]	Segmentation of puborectalis muscle and urogenital hiatus [119]	
Other organ systems or body location	Classification of pediatric pneumonia [120]	Improve US imaging contrast and detection rate [124]	Segmentation of subpleural pulmonary lesions [121]	
	Assessment and diagnosis of lung US [122,123]			

Note. US: ultrasound.

Shen YT, Chen L, Yue WW, Xu HX. Artificial intelligence in ultrasound. Eur J Radiol. 2021;139:109717. Epub 2021/05/08. doi: 10.1016/j.ejrad.2021.109717. PubMed PMID: 33962110.

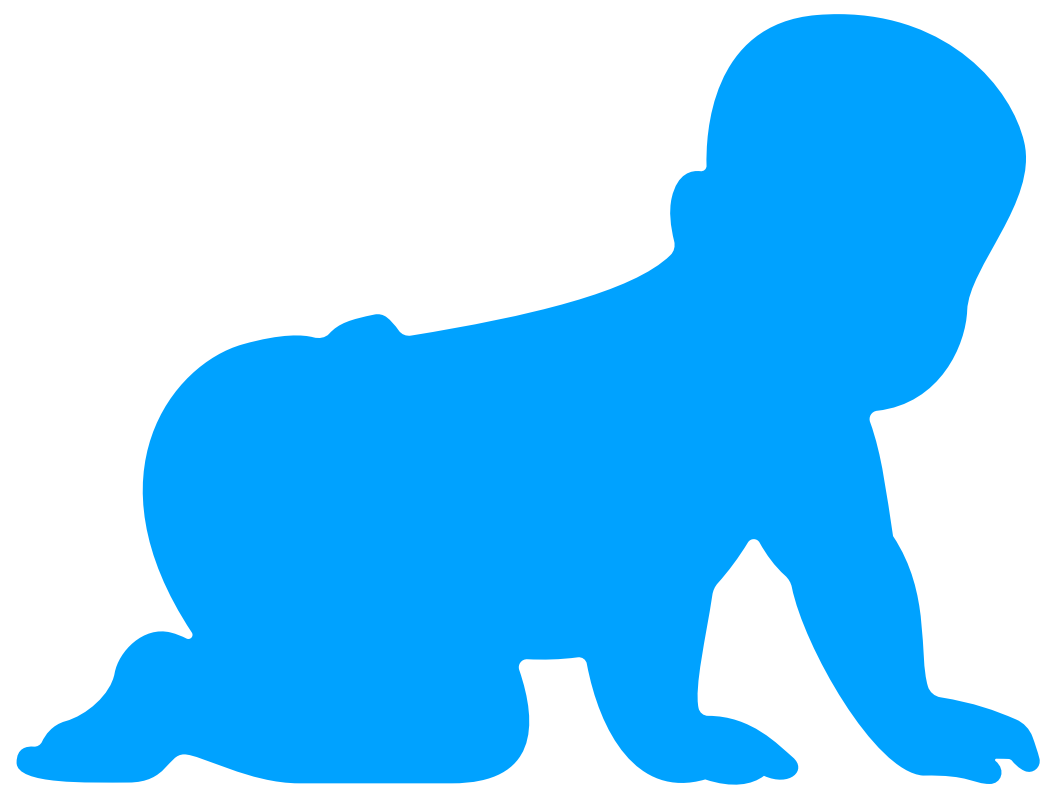


教師なし学習

異常検知



いつも吉野家  
たまに「すき家」



いつも吉野家  
吉野家好き

# 吉野家が甘さ吉野家を

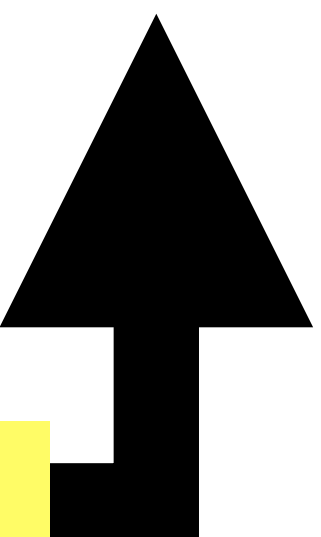
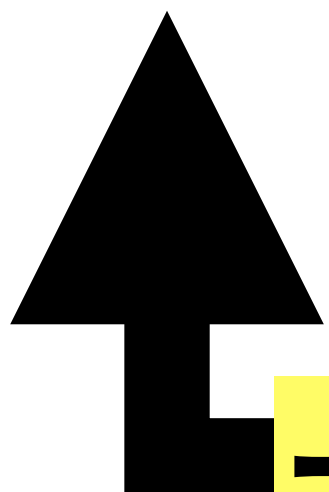
入力

醤油

想像



たまねぎ



一致していると大満足！

吉野家が  $\xrightarrow{a}$  吉野家を

$x$  入力



$a$  醤油

想像

$\hat{x}$



た シ タ ギ

$$E = \|x - \hat{x}\|$$

一致していると大満足！

$$x = f(x)$$

## Encode

画像をベクトルに変換して

$$\vec{a} = f(x)$$

画素数=次元数

画像よりも低い次元数

画像をベクトルに符号化

## Decode

変換したベクトルから  
再び画像に戻す

$$\hat{x} = g(\vec{a})$$

ベクトルから復元した画像

ベクトルを画像に復号化

その差がゼロに近ければ  
ベクトルは画像を効率よく  
表現している と言える

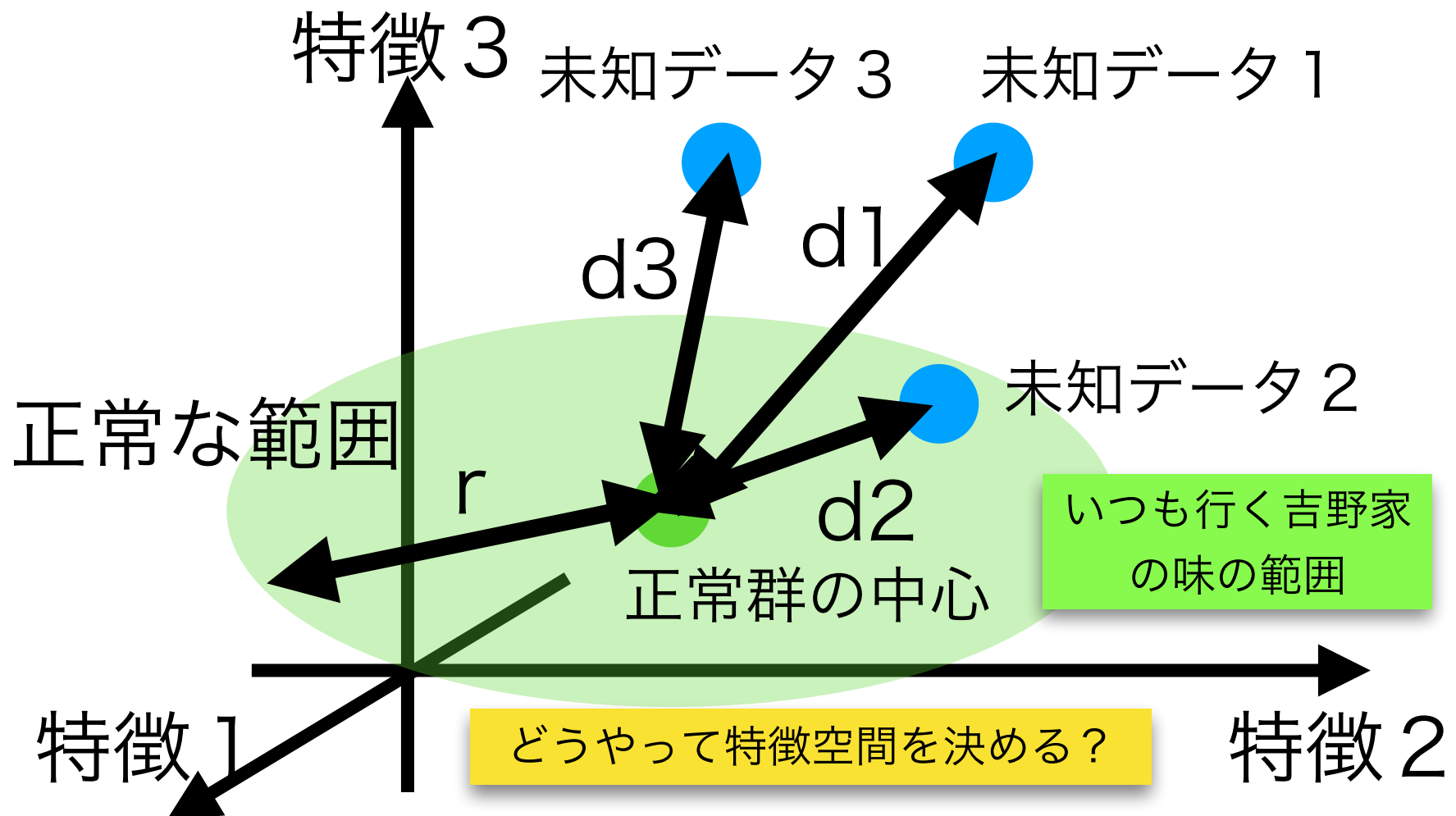
$$E = \|x - \hat{x}\|$$

自己複製の自己=Auto

元画像と復元画像の差

# 異常検知の考え方

範囲が決まれば そこからの逸脱で判定



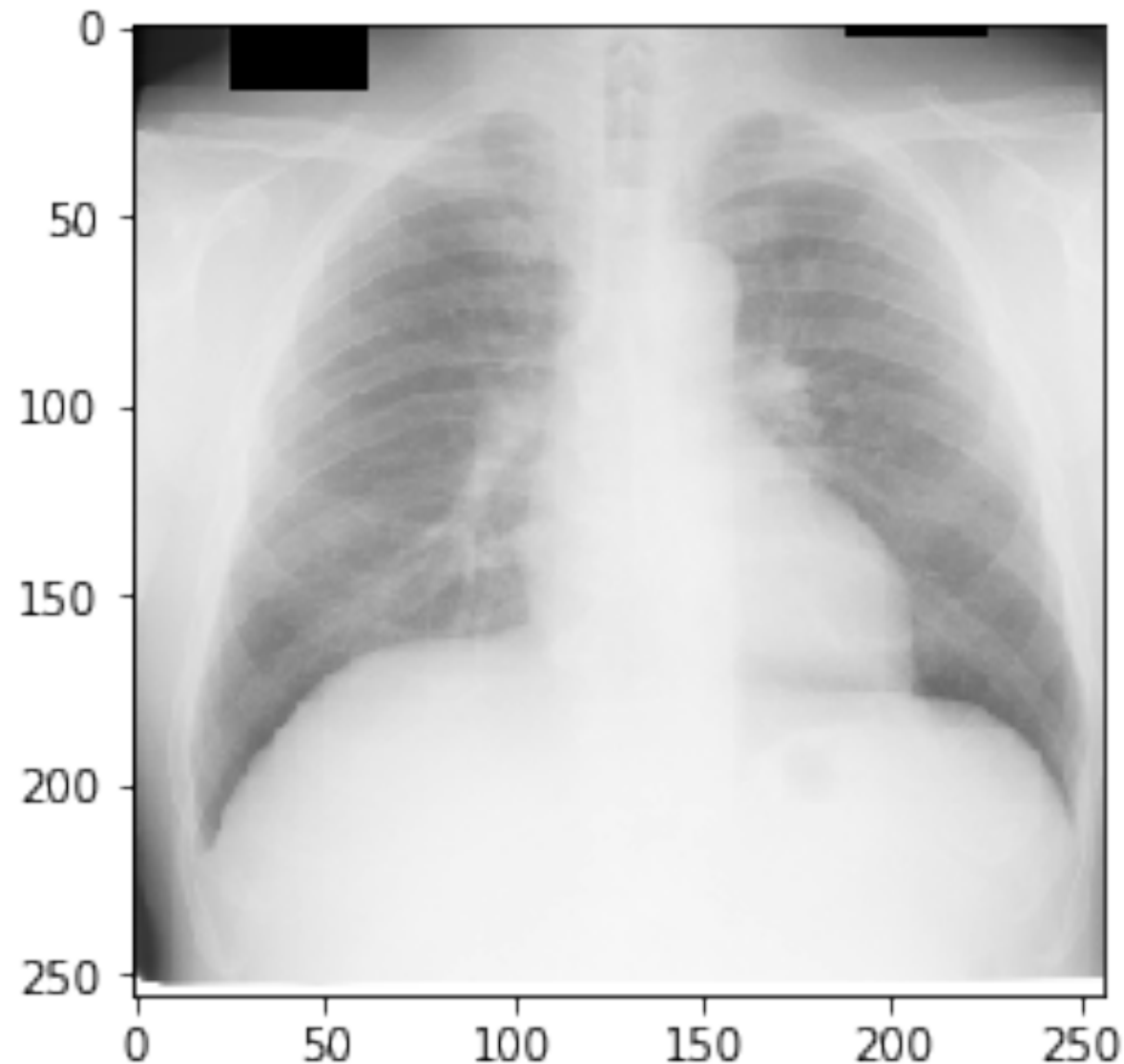
正常群から  
中心と範囲を決める

未知データと  
正常群の中心の  
距離を計算する

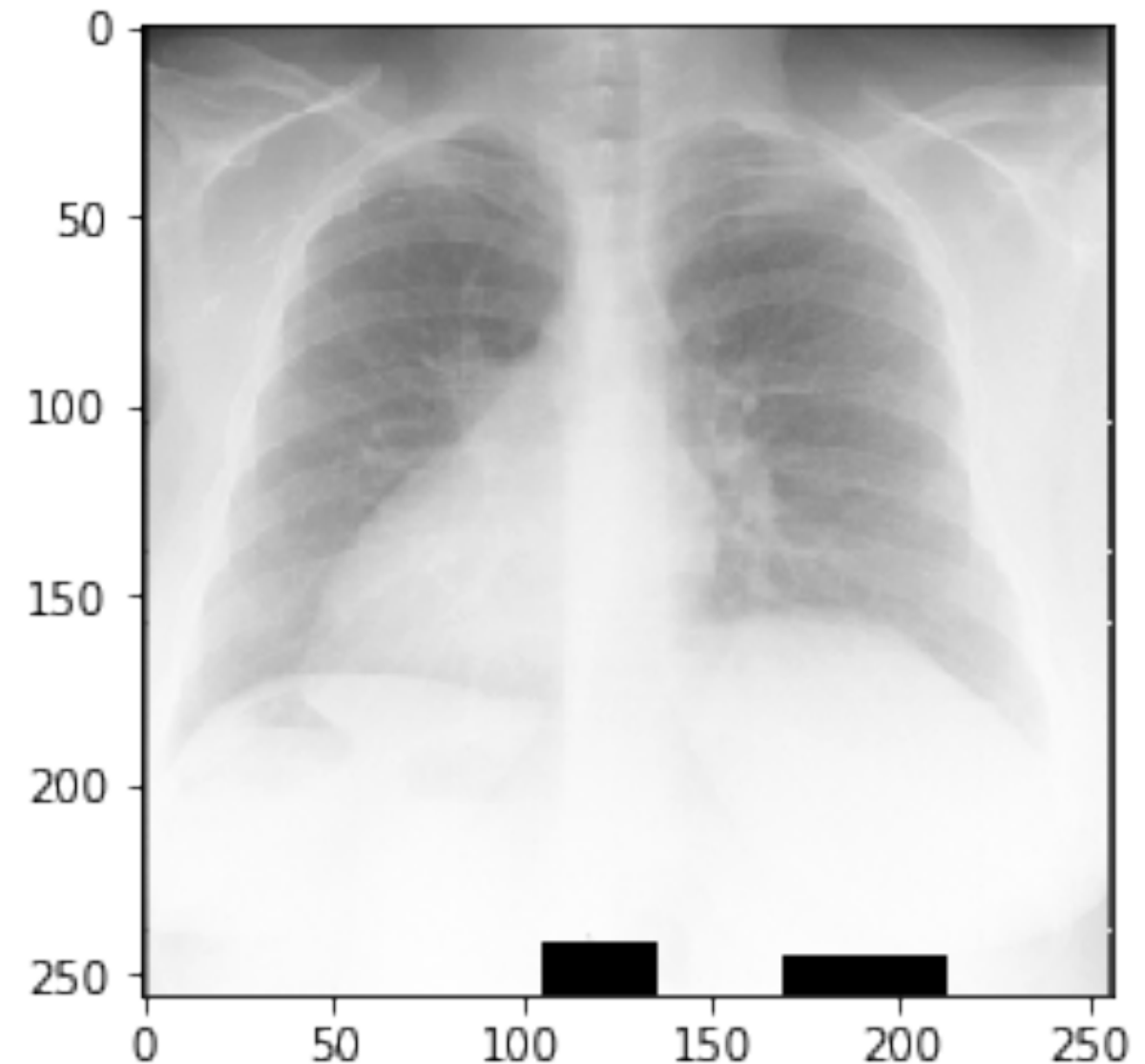
その距離が正常な  
範囲であるか  
判定する

$r < d_3 < d_1$ なのでデータ 1 と 3 は異常である

$d_2 < r$ なのでデータ 2 は正常である



正常像



反転像

65536次元

画像を入力

256x256画像=65536  
256x256x16=65536

128x128x32

64x64x64

32x32x128

8x8x256

4096次元 4x256=4096

8x8x256

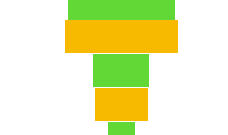
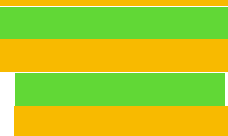
16x16x128

32x32x64

64x64x32

128x128x16

256x256x1



画素値



特徴



画素値

同じ画像を出力

(同じ=自己=Auto)

Layer (type)	Output Shape	Param #
conv2d_1 (Conv2D)	(None, 256, 256, 16)	160
max_pooling2d_1 (MaxPooling2)	(None, 128, 128, 16)	0
conv2d_2 (Conv2D)	(None, 128, 128, 32)	4640
max_pooling2d_2 (MaxPooling2)	(None, 64, 64, 32)	0
conv2d_3 (Conv2D)	(None, 64, 64, 64)	18496
max_pooling2d_3 (MaxPooling2)	(None, 32, 32, 64)	0
conv2d_4 (Conv2D)	(None, 32, 32, 128)	73856
max_pooling2d_4 (MaxPooling2)	(None, 16, 16, 128)	0
conv2d_5 (Conv2D)	(None, 8, 8, 256)	295168
max_pooling2d_5 (MaxPooling2)	(None, 4, 4, 256)	0
flatten_1 (Flatten)	(None, 4096)	0
reshape_1 (Reshape)	(None, 4, 4, 256)	0
conv2d_6 (Conv2D)	(None, 4, 4, 256)	590080
up_sampling2d_1 (UpSampling2)	(None, 8, 8, 256)	0
conv2d_7 (Conv2D)	(None, 8, 8, 128)	295040
up_sampling2d_2 (UpSampling2)	(None, 16, 16, 128)	0
conv2d_8 (Conv2D)	(None, 16, 16, 64)	73792
up_sampling2d_3 (UpSampling2)	(None, 32, 32, 64)	0
conv2d_9 (Conv2D)	(None, 32, 32, 32)	18464
up_sampling2d_4 (UpSampling2)	(None, 64, 64, 32)	0
conv2d_10 (Conv2D)	(None, 64, 64, 16)	4624
up_sampling2d_5 (UpSampling2)	(None, 128, 128, 16)	0
up_sampling2d_6 (UpSampling2)	(None, 256, 256, 16)	0
conv2d_11 (Conv2D)	(None, 256, 256, 1)	145
<hr/>		
Total params: 1,374,465		
Trainable params: 1,374,465		
Non-trainable params: 0		

65536次元

画像を入力

256x256画素=65536

256x256x16

128x128x32

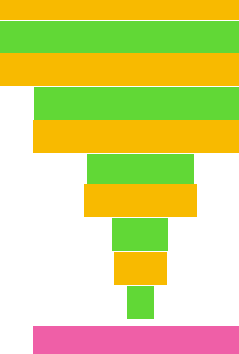
64x64x64

32x32x128

4096次元

8x8x256

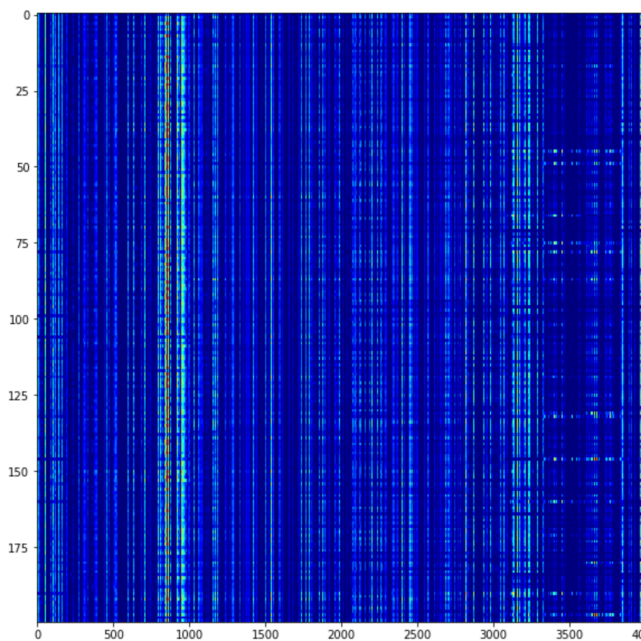
4x4x256=4096



画素値

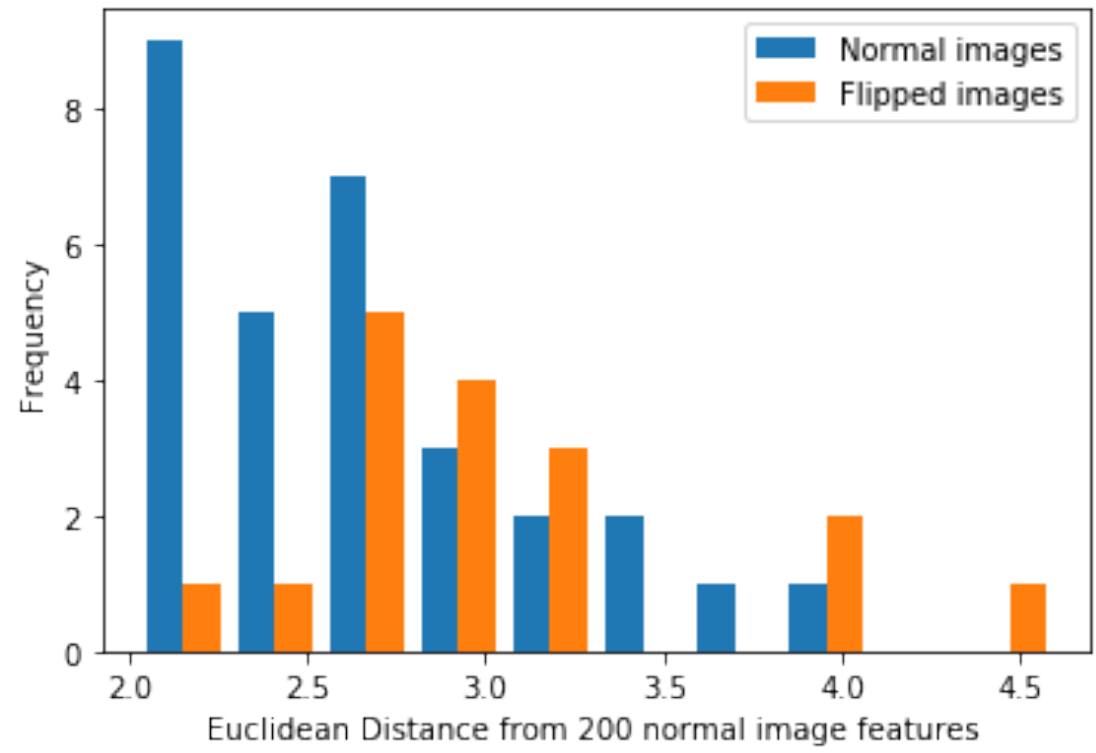


特徴

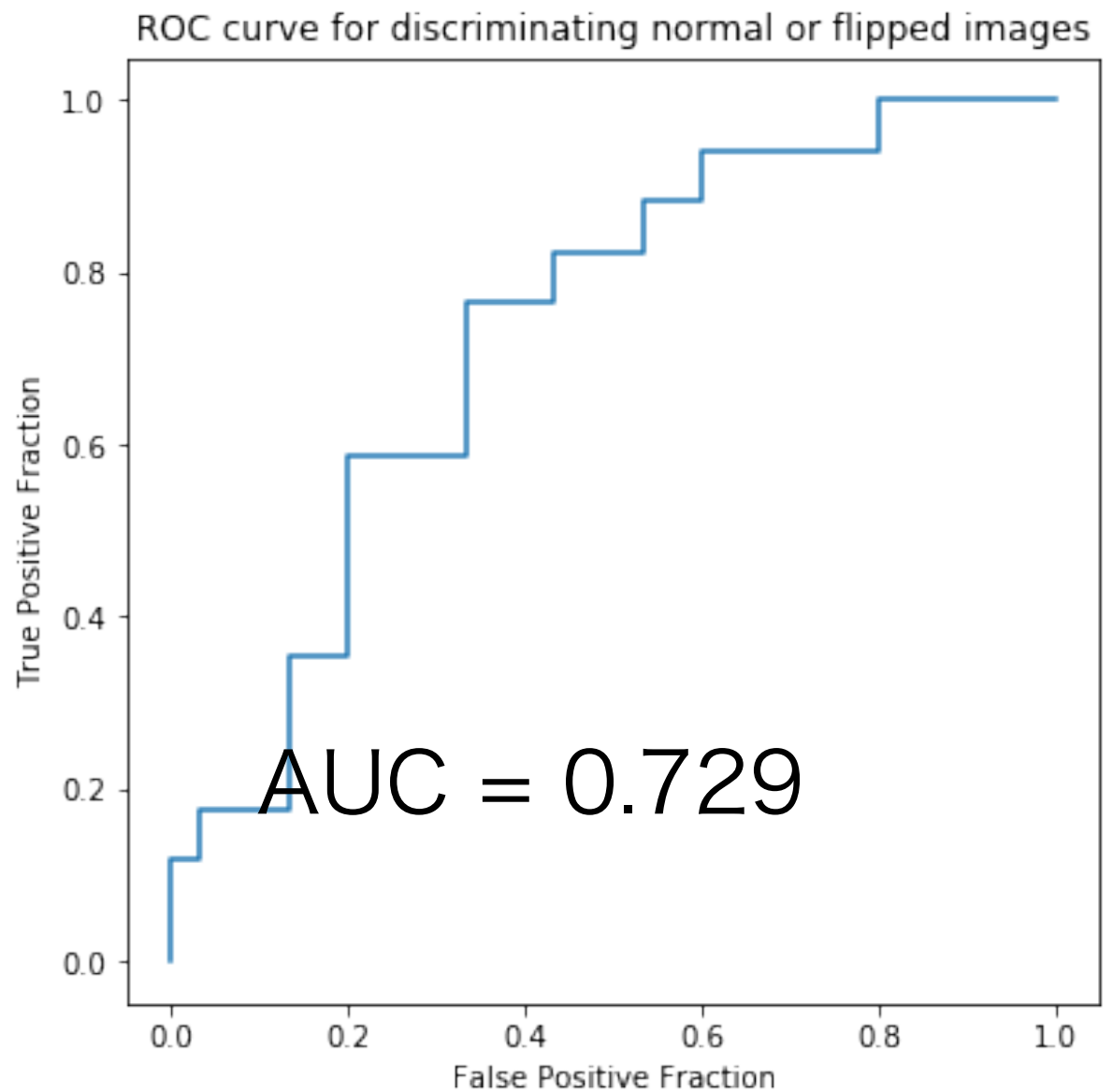


Layer (type)	Output Shape	Param #
<hr/>		
conv2d_1_input (InputLayer)	(None, 256, 256, 1)	0
<hr/>		
conv2d_1 (Conv2D)	(None, 256, 256, 16)	160
<hr/>		
max_pooling2d_1 (MaxPooling2)	(None, 128, 128, 16)	0
<hr/>		
conv2d_2 (Conv2D)	(None, 128, 128, 32)	4640
<hr/>		
max_pooling2d_2 (MaxPooling2)	(None, 64, 64, 32)	0
<hr/>		
conv2d_3 (Conv2D)	(None, 64, 64, 64)	18496
<hr/>		
max_pooling2d_3 (MaxPooling2)	(None, 32, 32, 64)	0
<hr/>		
conv2d_4 (Conv2D)	(None, 32, 32, 128)	73856
<hr/>		
max_pooling2d_4 (MaxPooling2)	(None, 16, 16, 128)	0
<hr/>		
conv2d_5 (Conv2D)	(None, 8, 8, 256)	295168
<hr/>		
max_pooling2d_5 (MaxPooling2)	(None, 4, 4, 256)	0
<hr/>		
flatten_1 (Flatten)	(None, 4096)	0
<hr/>		
Total params: 392,320		
Trainable params: 392,320		
Non-trainable params: 0		

同じ画像を出力  
(同じ=自己  
=Auto)

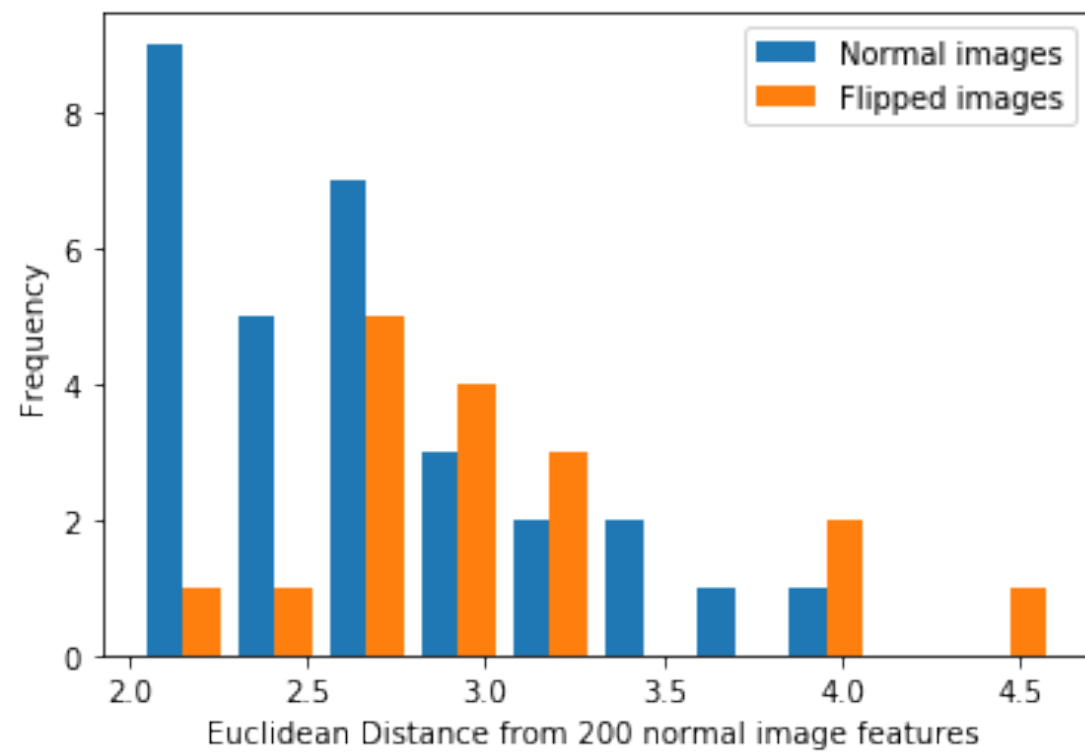


ユークリッド距離のヒストグラム

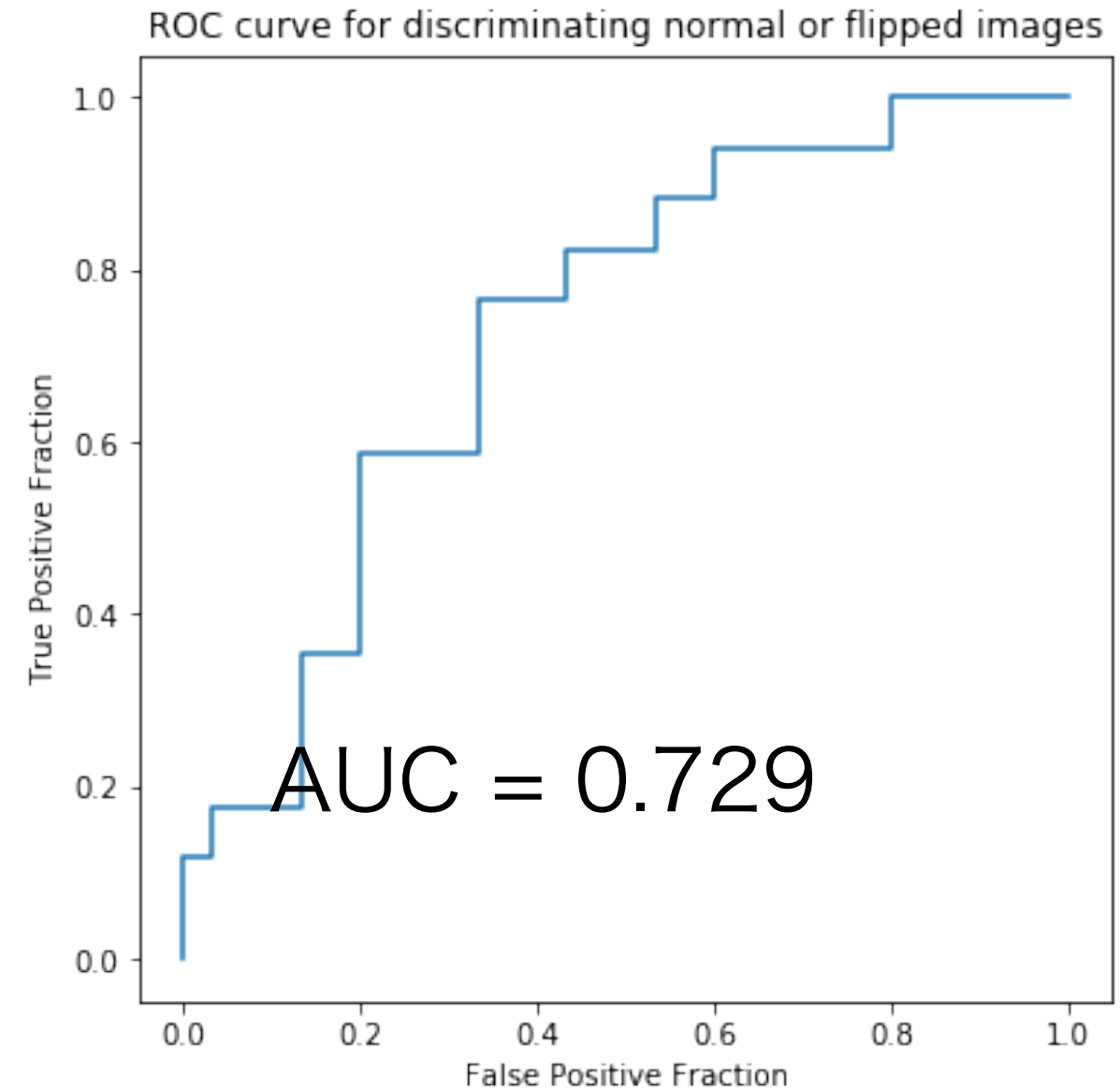


距離を確信度としたときのROC曲線

# データだけ集めて手法開発



ユークリッド距離のヒストグラム



距離を確信度としたときのROC曲線

# AutoEncoder & 異常検知

教師あり学習

代表例：画像分類

(問題点)

バランスよく学習データを  
集める必要がある

10例

1000例

通常：異常例は少なく、正常例は多い

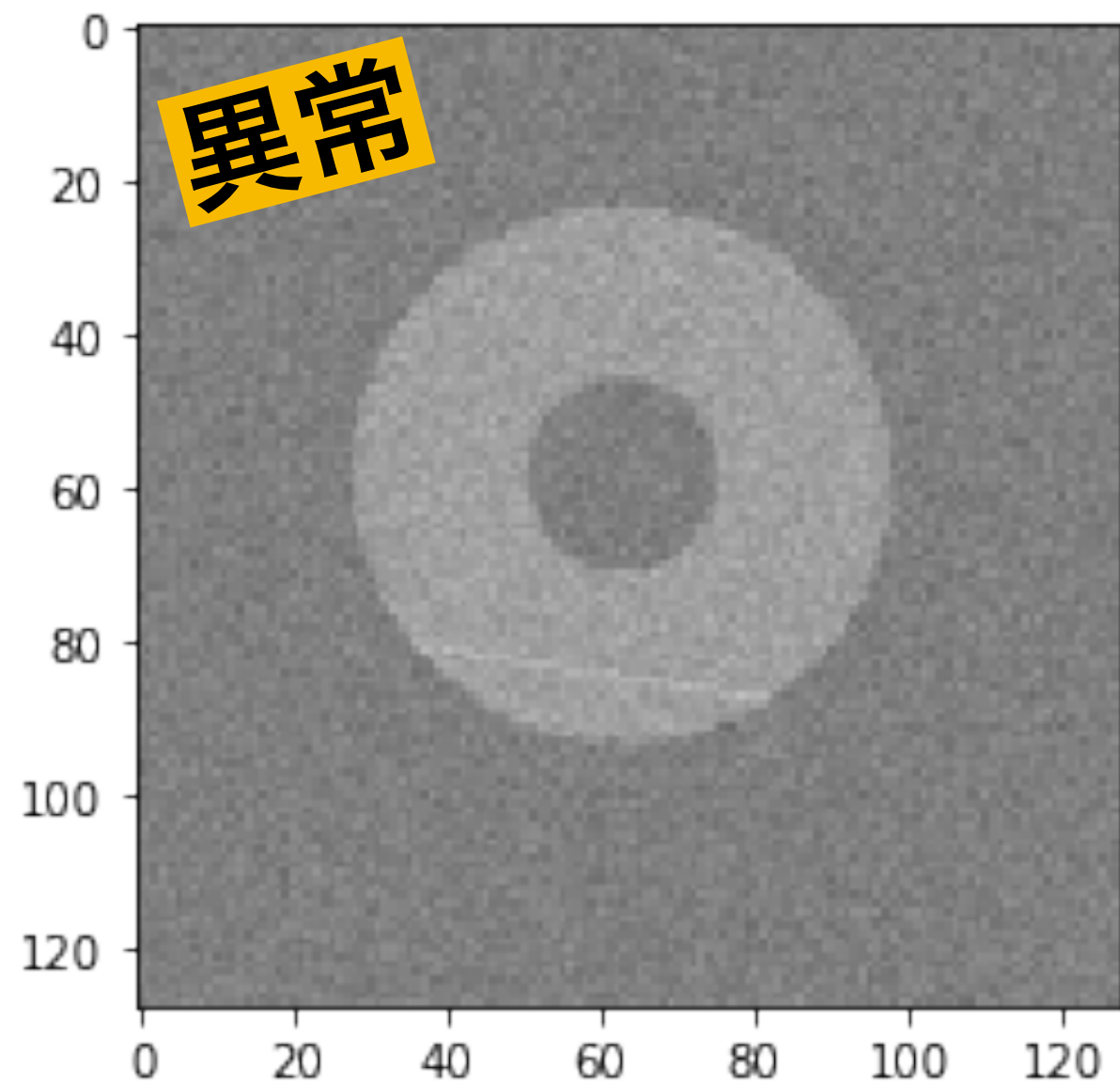
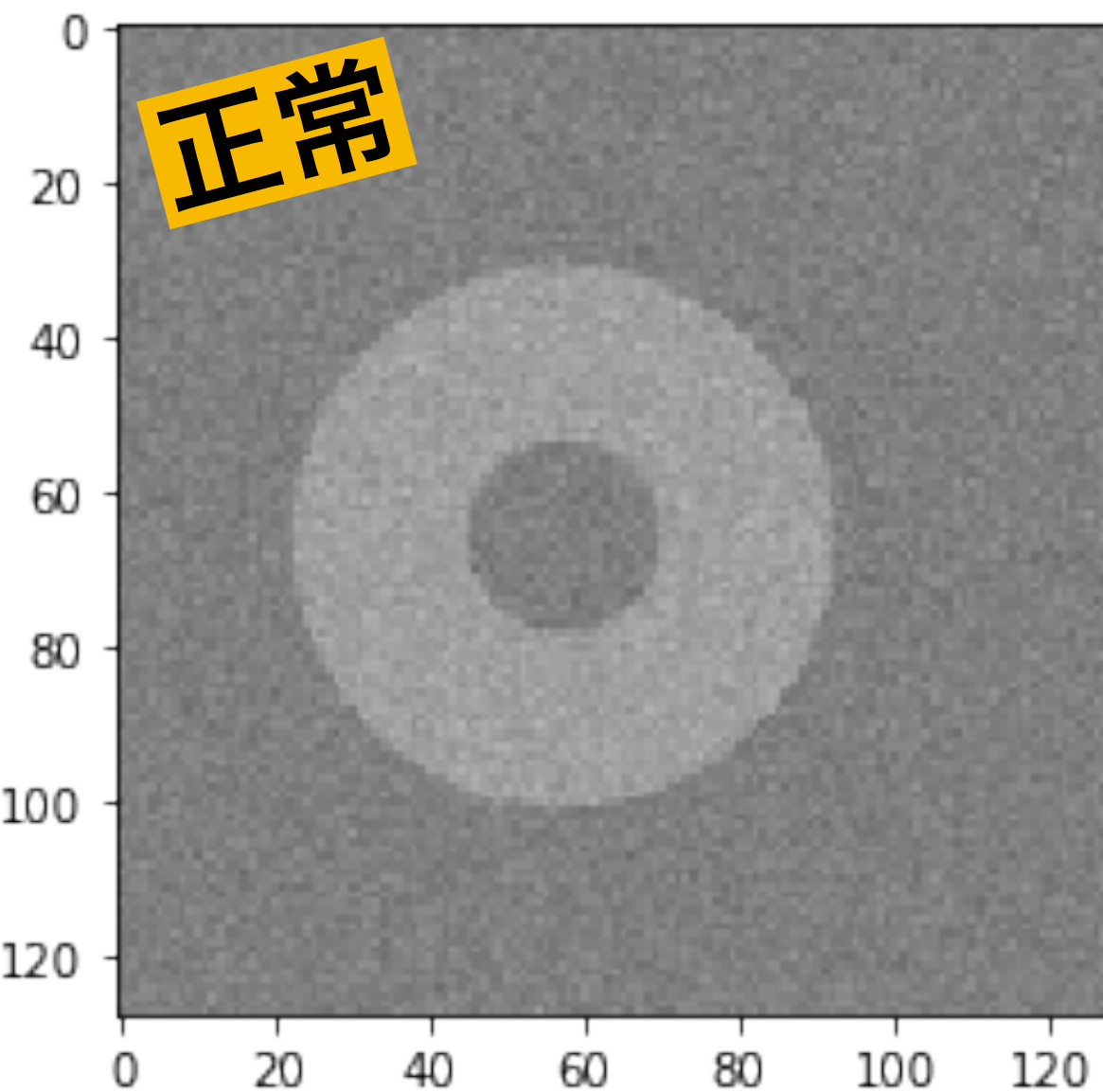
アンバランスが一般的

教師なし学習

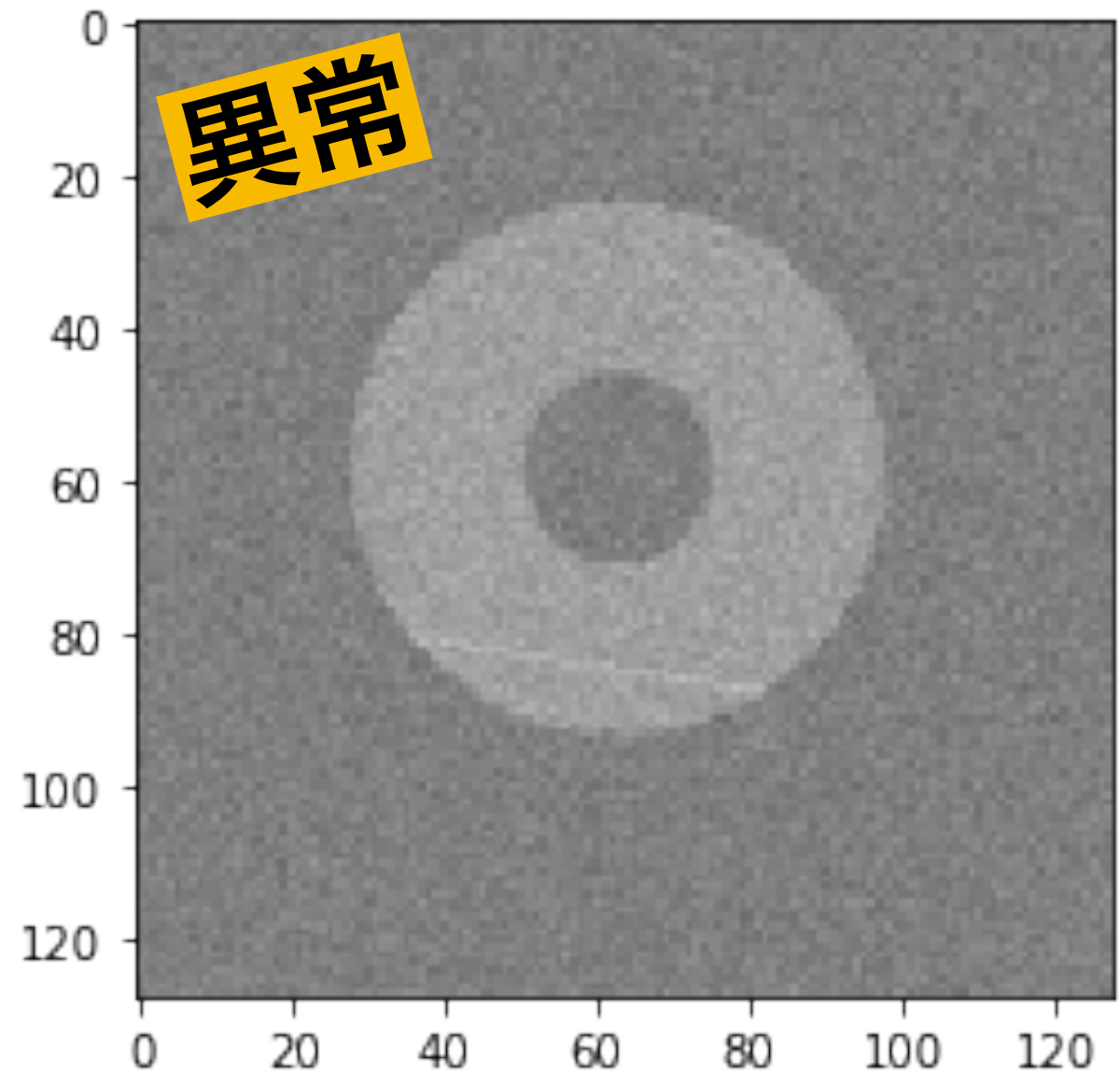
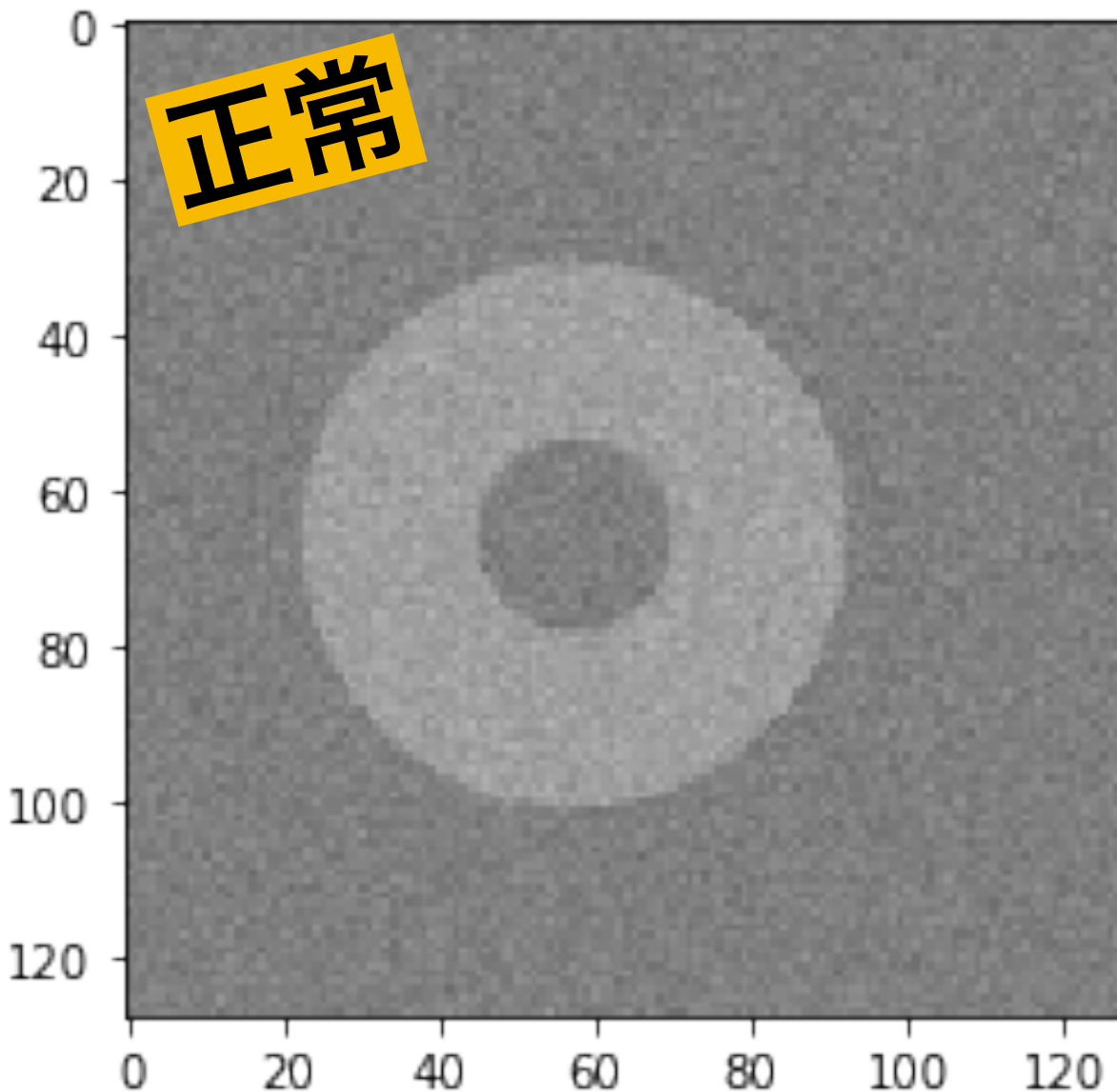
正常なデータのみから特徴抽出  
そのからの逸脱を定量化

逸脱の大きい場合を  
異常として検知

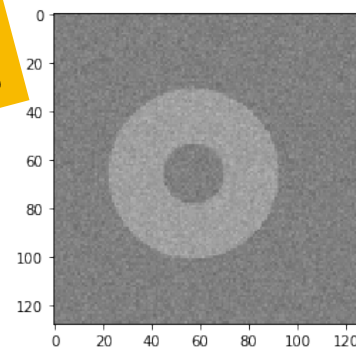
アンバランスなデータでも対応可能



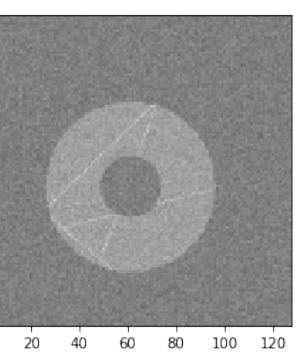
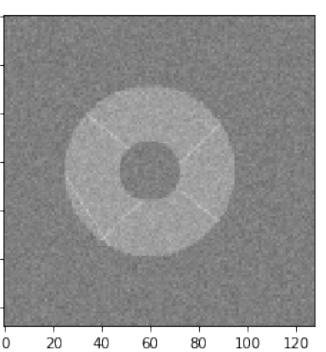
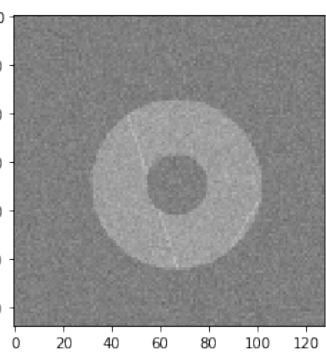
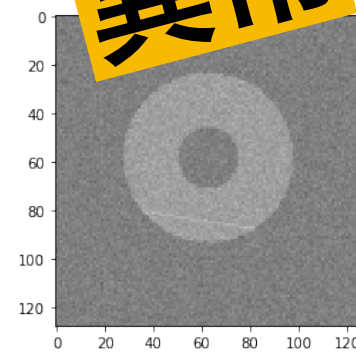
# データだけ集めて手法開発



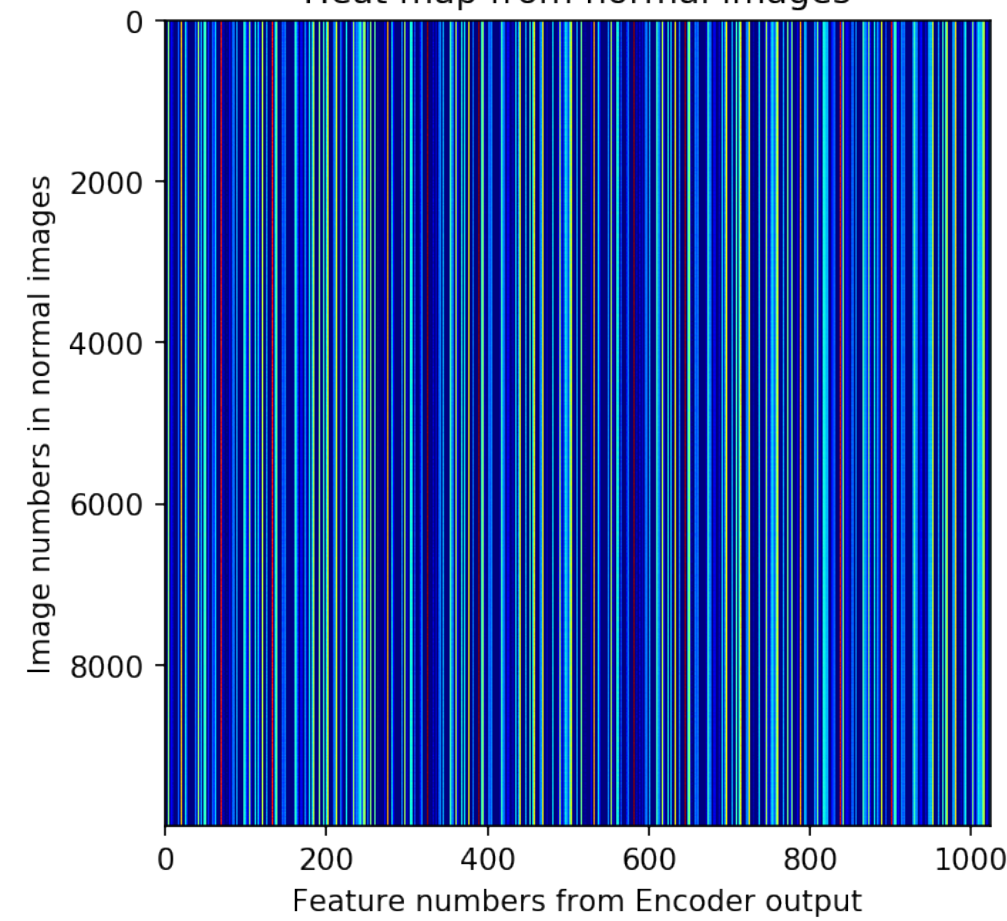
**正常**



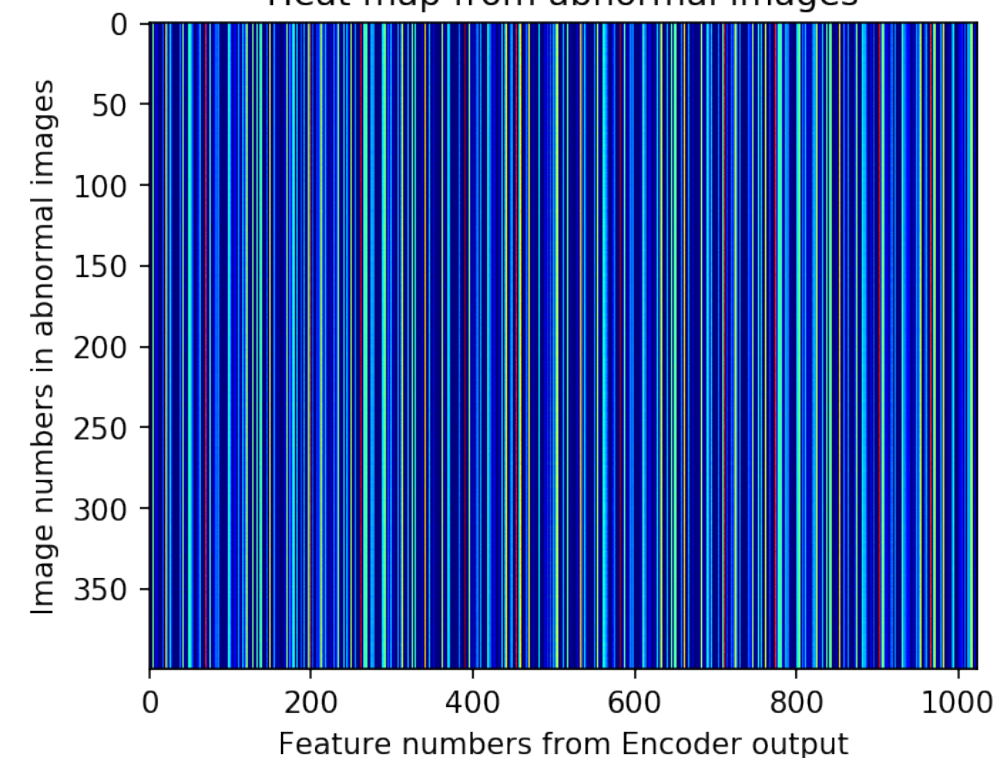
**異常**

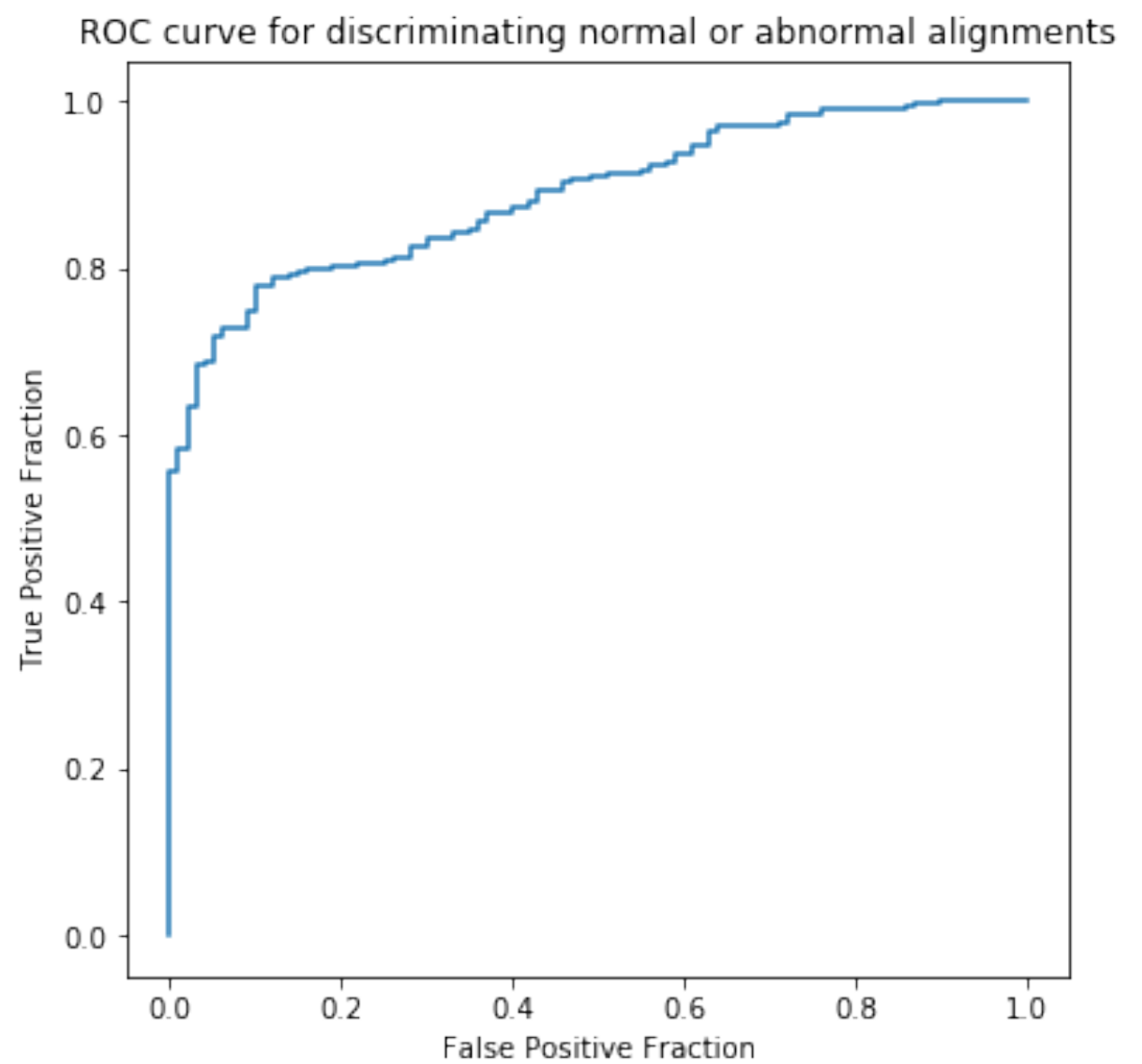
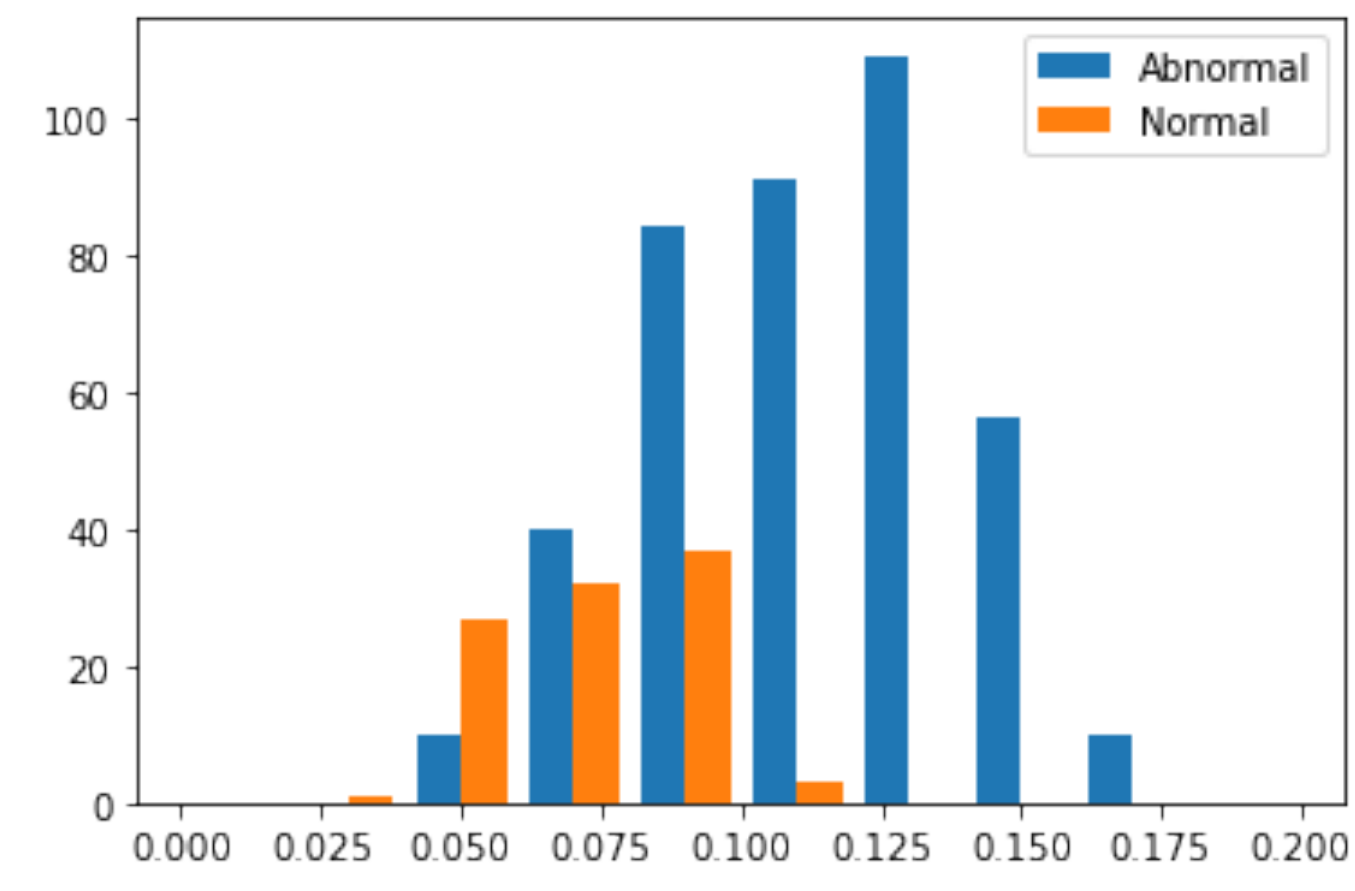


Heat map from normal images

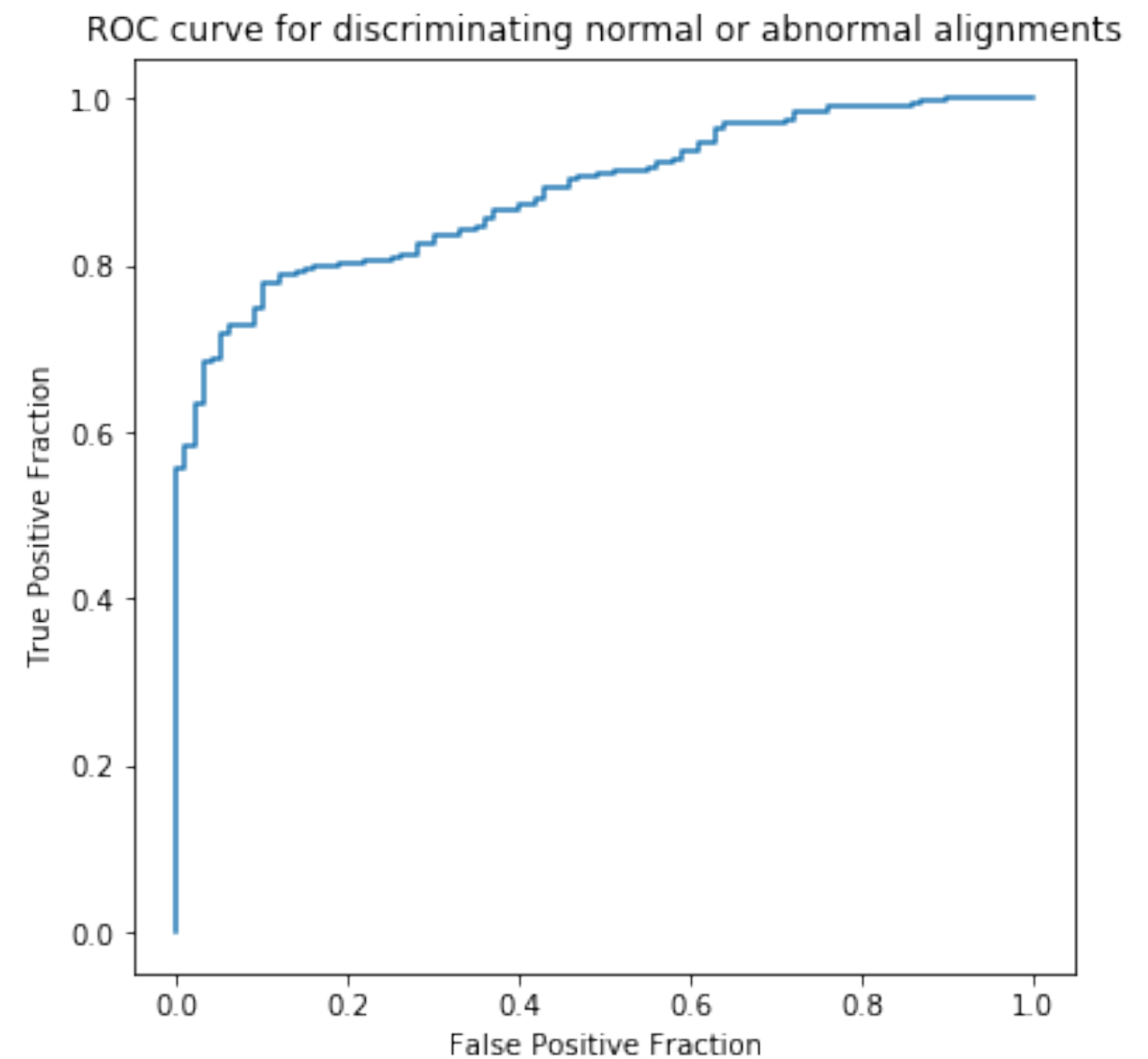
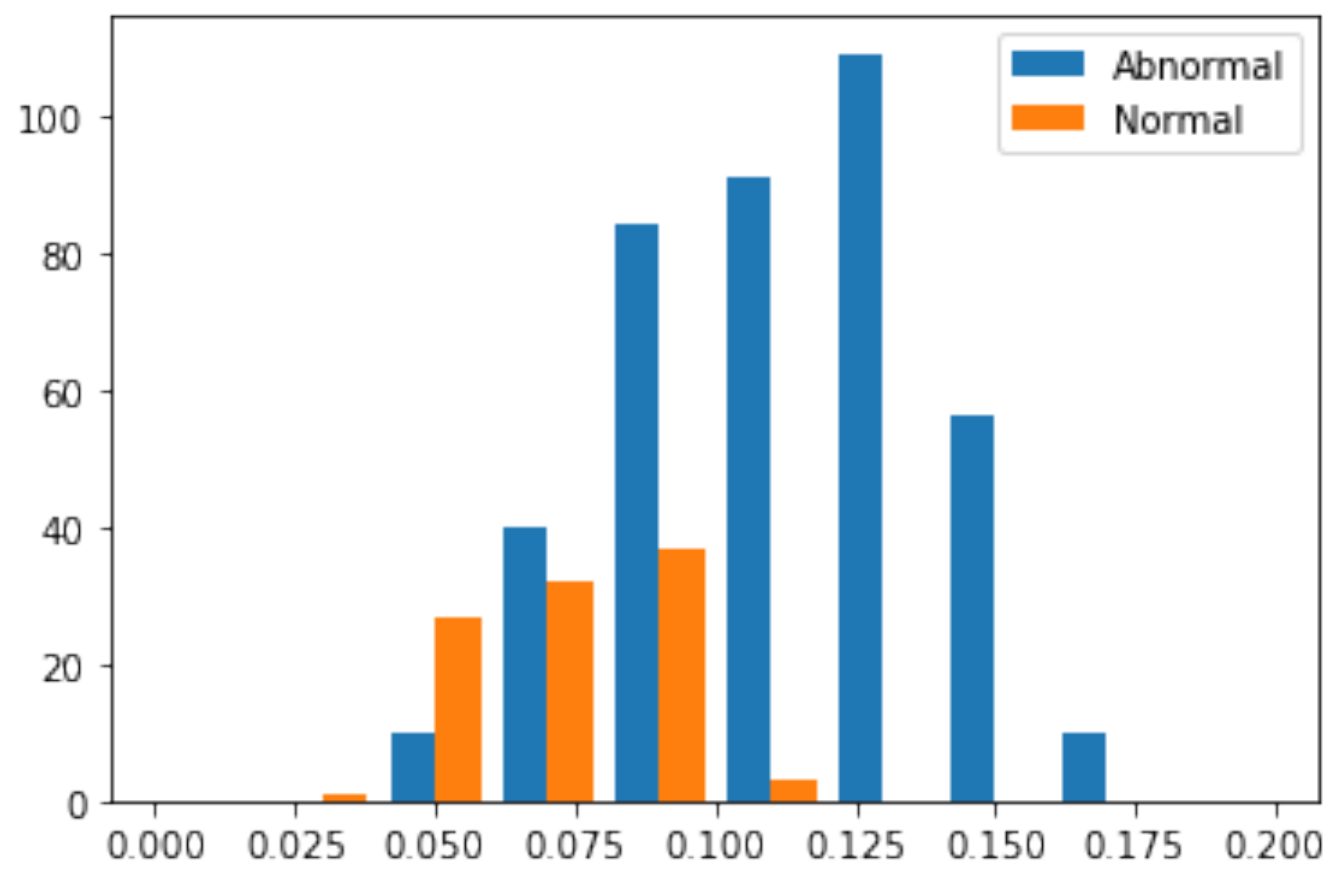


Heat map from abnormal images



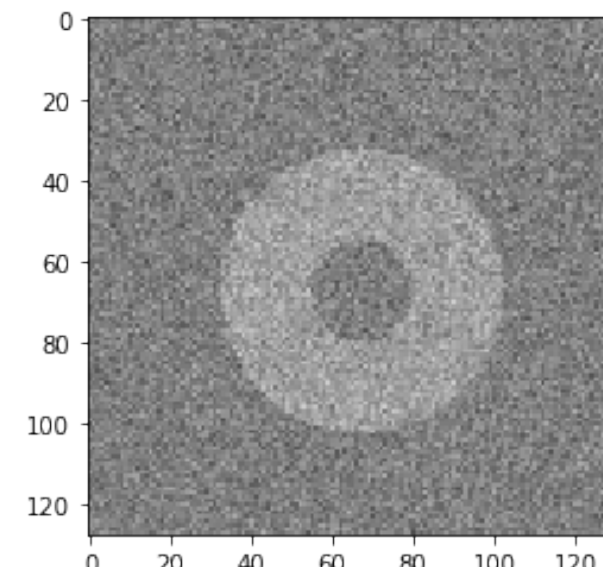


# データだけ集めて手法開発

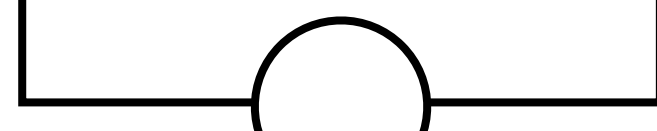
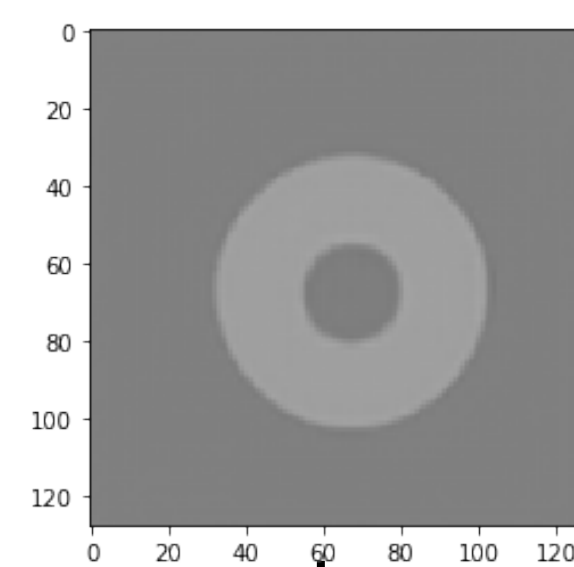


かっこよく言うとend-to-end

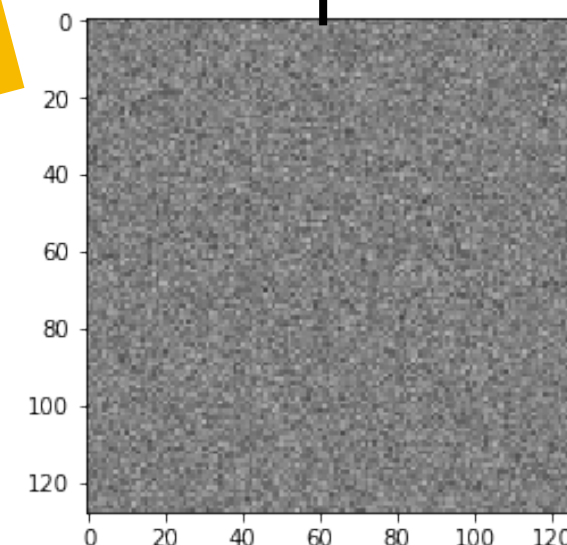
入力画像



AutoEncoderの出力画像

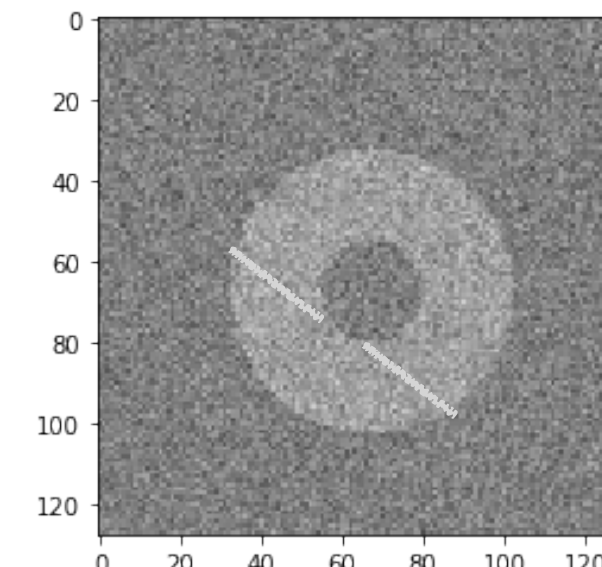


正常

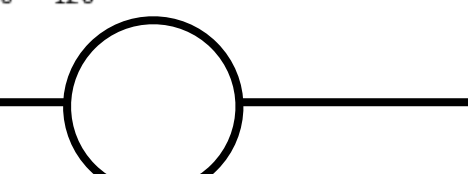
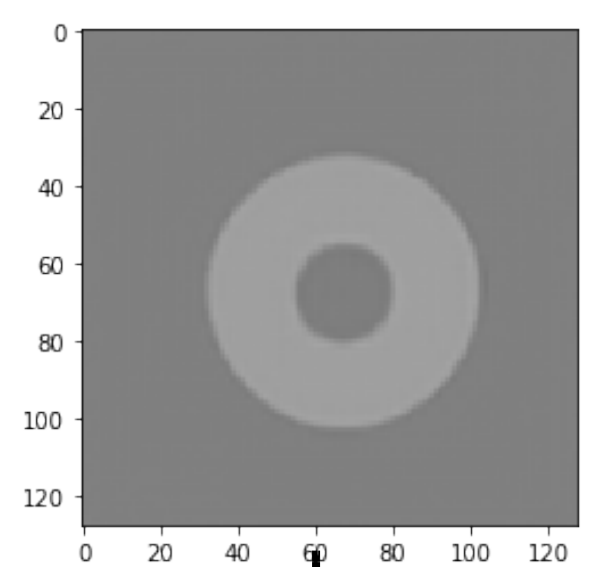


差分像

入力画像

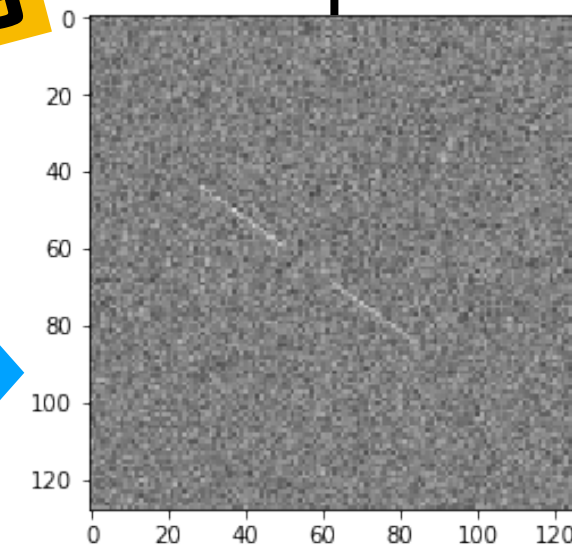


AutoEncoderの出力画像



異常

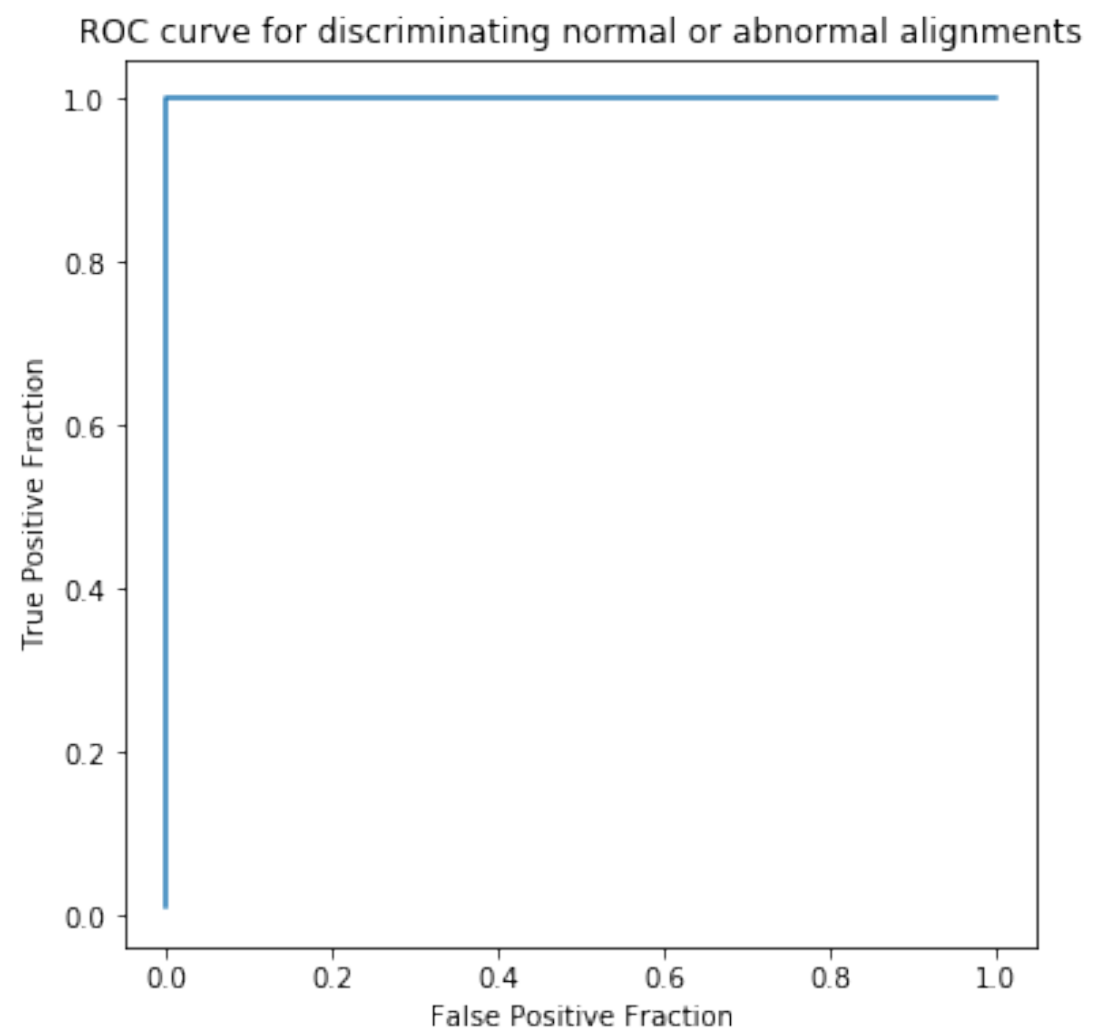
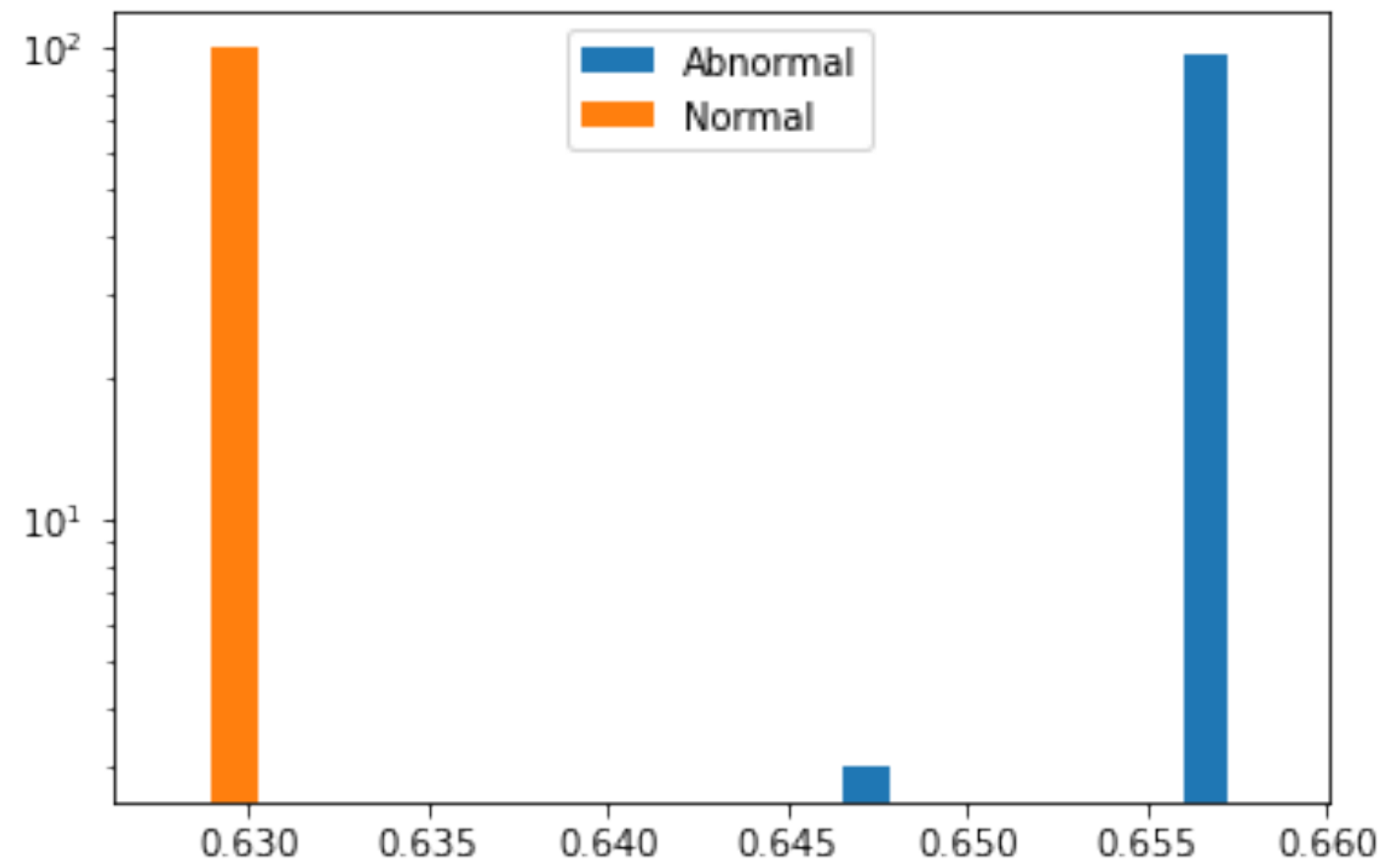
最大値に違いがあるかも？



差分像

極端な例ですが…

AutoEncoderを前処理としてうまく利用できれば  
単純な特徴量（例えば最大値）でも分離可能



といつても  
實際には  
簡単には  
うまくいきません

# まとめ

深層学習は、機械学習の方法の一つです。  
中でも「教師あり学習」が基本です。

機械学習は、データに基づいて課題を解きます。  
30~100例から実験できます。  
1000~10000例を目指としましょう。

人が学習するよりもたくさんの美味しい画像を食べさせないと深層学習は十分に成長しません。  
Garbage-in, garbage-outです（本当か？）